

Developing a System for Reliably and Predictably Generating, Recording, and Analyzing Flicker in Commercial and Residential Light Bulbs

A Thesis

Presented in Partial Fulfillment of the Requirements for the

Degree of Master of Science

with a

Major in Electrical Engineering

in the

College of Graduate Studies

University of Idaho

by

Eric Johnston

Approved by:

Major Professor: Brian K. Johnson, Ph.D., P.E

Committee Members: Herbert L. Hess, Ph.D., P.E.; Dennis M. Sullivan, Ph.D., P.E.

Department Administrator: Joseph D. Law, Ph.D., P.E.

December 2022

Abstract

Light bulb flicker has been an issue for as long as light bulbs have existed, and many negative health effects associated with light flicker have been well established and documented. Previous research has largely focused on flicker related to incandescent bulbs and on steady-state flicker behaviors. However, the increasing adoption of light-emitting diode (LED) bulbs, coupled with a growing prevalence of non-linear noise sources—such as switch-mode power supplies and variable frequency drives—is causing an increased need to better understand flicker behavior in a variety of bulb types. This thesis documents some of the basic principles of light measurement and flicker classification while also highlighting some of the relevant research into flicker behavior and IEEE guidance related to flicker. Having established a background in flicker behavior and measurement, this research then details the development of a physical testbed and python-based toolchain for generating, recording, analyzing, and displaying flicker behavior in several different bulb types. Finally, sample outputs are provided which demonstrate the ability of the testbed and toolchain to reliably and consistently conduct light flicker tests, record the results of those tests, and provide initial plotting and data analysis on the captured results.

Keywords: lightbulb, light bulb, LED, light-emitting diode, flicker, interharmonic, stroboscopic effect, IEC flickermeter, python, data capture, automation

Acknowledgments

On the academic side, I would like to express my sincere appreciation to my thesis committee, Dr. Brian Johnson, Dr. Herbert Hess, and Dr. Dennis Sullivan for their support, as well as the lessons they taught me in their classes. Specifically, I would like to thank Dr. Johnson for his advice, guidance, and help over the course of this research, it is all greatly appreciated.

On the professional side, I would like to thank Schweitzer Engineering Laboratories for sponsoring both my research and my education. Thank you to our department editor, Valerie Hudson for taking her own personal time to sift through my sea of haphazard capitalization and spacing and also for attempting to rein in my apparent love for commas. Thank you to my manager, Tracy Young, and my co-workers Ryan Thompson and Thomas Halstead for their help, feedback, and advice. In particular, I would like to express my appreciation to my friend and co-worker Joe Ferguson for all his help in coding, brainstorming, troubleshooting, tool development, and general sanity retention. I truly don't know how I would have gotten this thesis done without all the help and advice.

Dedication

Thank you so much for my wonderful wife, Brittany. I don't know what I would do without you, but it would definitely be a complete mess. You help me in so many different ways and I am so appreciative of all the love and support you have shown over the years. You help me stay on task, even when I don't want to, you keep me organized and motivated, and you take care of a thousand little things that I don't even know about. Thank you so much, I love you.

Thank you to my two boys, who have never known a time where Dad was not in grad school. Thank you to my family for the support and encouragement over the years. Finally, thank you to my friends for putting up with me complaining about grad school. I appreciate you all so very much.

Table of Contents

Abstract	ii
Acknowledgments	iii
Dedication	iv
Table of Contents	v
List of Tables	ix
List of Figures	x
Statement of Contribution	xii
Chapter 1: Introduction	1
Chapter 2: Background.....	2
2.1 Introduction	2
2.2 Types of Light Bulbs.....	2
2.2.1 Incandescent	3
2.2.2 Halogen	4
2.2.3 Compact Fluorescent Light (CFL)	4
2.2.4 Light-Emitting Diode (LED)	4
2.3 Light Measurement Basics	4
2.3.1 Introduction	4
2.3.2 Radiometric Quantities.....	5
2.3.3 Spectral Quantities.....	5
2.3.4 Photometric Quantities	6
2.3.5 Converting From Radiometric Quantities to Spectral or Photometric Quantities	8
2.3.6 Summary Of Quantities and Units.....	9
2.3.7 Relevance to Flicker Research	10
2.4 Flicker Background	11

2.4.1	Introduction To Flicker.....	11
2.4.2	Terms Associated with Light Flicker	12
2.4.3	Negative Effects of Flicker.....	12
2.4.4	Sources of Flicker.....	13
2.4.5	Flicker Classifications	14
2.5	Previous Research	18
2.5.1	Common Test Setup Configuration.....	18
2.5.2	Generalized Findings.....	21
2.5.3	Summary Of Previous Research.....	22
2.6	Background Summary	23
Chapter 3:	Test Setup.....	24
3.1	Introduction	24
3.2	National Instruments Data Acquisition Platform	24
3.2.1	What Is a DAQ?	24
3.2.2	DAQ Components	25
3.3	Test Fixture.....	30
3.3.1	Hardware Stages.....	31
3.4	Equipment List	34
3.5	Procedure for Conducting the Flicker Tests	35
3.5.1	Necessity of Bulb Warmup	35
3.5.2	Preprocessing: Signal Generation.....	35
3.5.3	Test Sequence	36
3.6	Summary	37
Chapter 4:	Development of the H5 Toolchain	38
4.1	Project Background	38
4.1.1	Initial Data Capture Tools “SELDAQ” And “NIPlay”	38
4.1.2	Why Use Python?	42

4.1.3	Why Use HDF5?	42
4.2	The Need for a New or Expanded Framework.....	43
4.2.1	Requirements for the Improved Framework	43
4.3	Combining Parts to Build a Versatile Test Toolchain.....	44
4.3.1	H5Model.....	45
4.3.2	H5Convert	45
4.3.3	H5Signalgen	45
4.3.4	H5NIDAQ	46
4.3.5	H5Plot.....	46
4.3.6	H5Tools	46
4.4	Conclusion.....	47
Chapter 5:	Results	48
5.1	Introduction	48
5.2	Explanation of Measurements for Thorlabs Light Sensor.....	48
5.3	Data Capture and Plotting	49
5.3.1	Common Test Attributes	50
5.3.2	Frequency Sweep.....	51
5.3.3	Frequency Toggle.....	56
5.3.4	Single Tone Injection	62
5.4	Conclusion.....	69
Chapter 6:	Summary, Conclusion, and Future Work	70
6.1	Summary	70
6.2	Conclusion.....	70
6.3	Future Work	70
6.3.1	Analyzing Flicker Characteristics of Various Bulb Types.....	70
6.3.2	Improving Test Fixture to Allow for More Accurate Energy Measurement.....	71
6.3.3	Ongoing Improvements to the H5 Toolchain	71

6.3.4	Validate IEEE Flicker Guidance	71
6.3.5	Increased Current Draw on CFL and LED Bulbs When Exposed to Noise	72
6.3.6	Asymmetric Data on Some of The Captures	72
	Bibliography	73
	Appendix A: The H5 Tool library	78
A.1	H5 Model	78
A.2	H5 Signal Generator	80

List of Tables

Table 1: Applicable Units at Different Stages in the Test Sequence.....	11
Table 2: Summary of prior research.....	20
Table 3: DAQ Module Categories.....	28
Table 4: Equipment List.....	34
Table 5: Advantages and Disadvantages of Different Data Storage File Types	42
Table 6: Frequency Sweep Noise Signals	51
Table 7: Frequency Toggle Noise Signals.....	56
Table 8: List of Single Tone Injection Frequencies	62

List of Figures

Figure 1: Feit Electric 100 W Incandescent Bulb [1]	3
Figure 2: GE Lighting 60 W Halogen Bulb [2].....	3
Figure 3: Great Value 9 W LED Bulb [3]	3
Figure 4: GE Lighting 23 W CFL Bulb [4].....	3
Figure 5: Light Bulb Color Temperature Chart [10]	7
Figure 6: Gigahertz-Optic Table of Fundamental Units, Part 1. [9].....	9
Figure 7: Gigahertz-Optic Table of Fundamental Units, Part 2 [9].....	9
Figure 8: Spectral Response of Several Different Kinds of Light Bulbs [12].....	10
Figure 9: Flicker Classifications [13]	15
Figure 10: IEEE Flicker Guidelines [13].....	18
Figure 11: Generic Light Flicker Test Setup	19
Figure 12: Example of Circuit Topology and Flicker Response of Two Different LED Drivers [26].	21
Figure 13: Examples of Flicker Response for Various Types of Bulbs [16].....	22
Figure 14: Example of a Single-Slot vs. Multi-Slot DAQ Chassis [28].....	26
Figure 15: Example of Some of the Module Options Available [28].....	27
Figure 16: Test Fixture Diagram	30
Figure 17: Flicker Test Fixture.....	31
Figure 18: Techron Bridged-Mono Configuration	32
Figure 19: Test Sequence	36
Figure 20: SELDAQ Tool [40].....	39
Figure 21: NIPlay Tool [40]	40
Figure 22: Time Domain Capture for Incandescent Frequency Sweep.....	52
Figure 23: Time Domain Capture for All Light Channels During Frequency Sweep Test.....	53
Figure 24: Time Domain Capture for All Current Channels During Frequency Sweep Test	54
Figure 25: Spectral Response for All Light Channels During Frequency Sweep Test	55
Figure 26: Time Domain Capture for Incandescent Frequency Toggle	57
Figure 27: Time Domain Capture for All Light Channels During Frequency Toggle Test.....	58
Figure 28: Spectral Response for All Light Channels During Frequency Toggle Test.....	59
Figure 29: 10 Hz DFT for All Light Channels During Frequency Toggle Test.....	60
Figure 30: 20 Hz DFT for Individual Light Channels During Frequency Toggle Test.....	61
Figure 31: Time Domain Response to 70 Hz Injected Noise for All Bulb Light Channels	63
Figure 32: Spectral Response for All Light Channels During 70 Hz STI Test.	64

Figure 33: Frequency Response of CFL Bulb Light Output to Different Injected Tones	65
Figure 34: Frequency Response of Halogen Bulb Light Output to Different Injected Tones	66
Figure 35: Frequency Response of Incandescent Bulb Light Output to Different Injected Tones	67
Figure 36: Frequency Response of LED Bulb Light Output to Different Injected Tones.....	68
Figure 37: Example Signal.JSON Template.....	81

Statement of Contribution

The development of the H5 toolchain was a collaborative effort, and the primary contributors for each of the individual tools were as follows: H5Model: Thomas Halstead; H5Convert: Ammon Kunsler and Joe Ferguson; H5Signalgen: Eric Johnston, Joe Ferguson, and Tracy Young; H5NIDAQ: Eric Johnston, Joe Ferguson, and Tracy Young; H5Plot: Eric Johnston and Joe Ferguson; H5Tools: Eric Johnston and Joe Ferguson.

Chapter 1: Introduction

The original goal of this research was to gain a better understanding of what types of power system noise or disturbances would be most likely to cause undesirable or unsafe levels of flicker in an office or manufacturing setting. This research was sponsored by Schweitzer Engineering Laboratories, Inc. (SEL), with the intention of understanding potential hazards to employees, either in an office or manufacturing environment. The primary concern in both cases related to the risk of headache, epileptic seizures, or other negative health effects on employees. Researchers at SEL expressed a desire to have a way to determine if there were any kinds of power system disturbances or noise sources that would be likely to cause negative health effects. The identification of “troublesome” disturbances or noise behaviors would then allow SEL to evaluate if such behaviors were present in the power systems for the company’s office and factory environments, as well as if any mitigation steps were necessary. The primary challenge for this research came from creating a test setup capable of reliably testing, recording, and analyzing flicker behavior. As the research progressed, the focus of the research shifted from understanding and analyzing flicker to creating a set of tools for performing the analysis and testing.

The updated objective of this thesis is to develop a testbed and software toolchain capable of conducting light flicker tests. The testbed needs to be able to output pre-defined test signals, amplify the signal to a voltage compatible with the bulb under test, and record both the input and relative output values of the test system. The toolchain needs to be capable of generating test sequences, running the tests, capturing the resultant values, processing the captured data values, and graphing or otherwise displaying the results. In order to increase reliability and repeatability, the toolchain also needs to be scriptable, so that a set of tests could be defined and then run sequentially for each bulb and test combination.

Chapter 2 provides an introduction to light and flicker measurement, as well as a summary of previous research into lighting flicker. Chapter 3 describes the physical testbed setup and the sequence for conducting a set of flicker tests. Chapter 4 details the development of the software toolchain for conducting tests. Chapter 5 demonstrates the functionality of both the testbed and toolchain by providing outputs and observations from various example test sequences. Chapter 6 summarizes the results of this thesis and highlights topics for future research.

Chapter 2: Background

2.1 Introduction

In order to be able to study light flicker or conduct meaningful tests, it is first necessary to understand the fundamental concepts associated with lighting, light bulbs, flicker, and light measurement.

Section 2.2 describes the different types of light bulbs that were used in this research, as well as their basic principles of operation. Section 2.3 provides an introduction to light measurement. Section 2.4 discusses the effects, causes, and classification of lighting flicker. Finally, section 2.5 discusses previous research on the topic of lighting flicker and discusses the primary components of a flicker testbed setup.

2.2 Types of Light Bulbs

Examples of the different types of light bulbs used in this research are shown in Figures 1-4. Figure 1 shows a 100 W incandescent bulb, Figure 2 is a 60W halogen bulb, Figure 3 is a 9 W light-emitting diode (LED) bulb, and Figure 4 is an 11 W compact fluorescent (CFL) bulb. With the exception of Figure 4, all of the bulbs shown are the product image for the actual bulbs used in the test. The image for Figure 4 was chosen because it more clearly demonstrates the “helix” shape that is commonly associated with CFL bulbs, whereas the CFL used for testing has an additional layer in its construction that gives it a more traditional bulb shape.

Figure 1: Feit Electric 100 W Incandescent Bulb [1]



Figure 2: GE Lighting 60 W Halogen Bulb [2]



Figure 3: Great Value 9 W LED Bulb [3]



Figure 4: GE Lighting 23 W CFL Bulb [4]



2.2.1 Incandescent

Incandescent bulbs are the “traditional” form of implementing electric lighting. The principle of operation for an incandescent bulb is to send current through a thin filament of wire, which then heats up to the point of emitting visible light [5]. Typically, this filament is made of tungsten [6], though other materials have been used in the past. Historically speaking, most light bulbs have been incandescent bulbs, and most bulbs available in stores will list their light output compared to some equivalent incandescent bulb wattage (e.g., 40 W equivalent, 60 W equivalent, 100 W equivalent, etc.).

2.2.2 Halogen

Halogen bulbs operate on a similar principle to incandescent, with the exception that a given bulb will contain a smaller, inner bulb filled with halogen. When the tungsten molecules from the filament evaporate, they interact with the halogen in a way that causes the molecules to recombine with the filament, instead of depositing elsewhere on the bulb. This recombination mechanism allows the filament to be much hotter, which in turn produces more light for a given wattage [5].

2.2.3 Compact Fluorescent Light (CFL)

Compact fluorescent lights operate by energizing a gas-filled tube to the point that the individual gas molecules become excited and begin emitting photons. Typically, these photons are in the ultraviolet (UV) range and would not be useful for lighting purposes. However, the inner wall of the tube contains a phosphorescent coating that reacts with the UV photons to produce visible light. CFL bulbs are typically much more energy efficient than halogen or incandescent bulbs [5] [7].

2.2.4 Light-Emitting Diode (LED)

Light-emitting diode (LED) bulbs operate by applying energy to one or more individual LED cells to generate photons. The light-emitting diodes themselves are constructed from specially formulated semiconductor materials. When energy is properly applied to the diode, the energy directly stimulates electrons in the material and causes them to “jump” between energy levels in the material and emit photons (the specifics of electron energy levels, semiconductor formulation, and photon generation are outside of the scope of this paper) [8]. LED bulbs are generally the most efficient bulb type.

2.3 Light Measurement Basics

2.3.1 Introduction

One of the first challenges that needed to be addressed in this research was gaining an intuitive understanding of what exactly is to be measured and how those measured values relate to the voltage and current inputs of the various light bulbs under test. The following sections cover the basics of light measurement, what the various quantities mean, and how to convert from one set of quantities to another.

2.3.2 Radiometric Quantities

Radiometric quantities deal with energy—either radiating from, or incident on—an object over time. The units associated with radiometric quantities are ones that are frequently used in electrical engineering (e.g., joules, seconds, watts, meters, etc.). Radiometric quantities are indicated by a subscript e, for "energy" (e.g., Φ_e and E_e).

The concepts associated with radiometry are ones that come up in other branches of the electrical engineering field. For example, the concept of irradiance—or the amount of power incident on a surface per unit area—is directly applicable when evaluating a location for installing solar panels [8].

Radiometric quantities do not take the spectral response of a given object or surface into account, nor are they affected by any sort of biological response. Instead, they represent a sum of all the radiated, absorbed, or reflected power across the entire spectrum [9]. Obviously, this presents an incomplete picture, as the spectral response of an object or surface depends on the amount of energy emitted or absorbed from a given light source. An example of the importance of spectral response is to look at the absorption capabilities of solar panels. The semiconductor material used in the construction of the panel directly affects what frequencies of energy it can absorb, and if the designers of a solar panel want to widen the range of absorption, they must add in different kinds of semiconductors. Solar panels cannot convert light energy outside of a certain frequency range, and that range is defined by the chemical makeup of the panel's semiconductor material [8].

2.3.2.1 Relevant Radiometric Terms

Radiant Power/Radiant Flux, Φ_e : The total power of radiation emitted by a source, transmitted through a surface, or impinging upon a surface. Radiant power is measured in watts (W) [9].

Isotropic Light Source: A light source that emits uniformly in all directions.

Irradiance E_e : The amount of radiant power impinging upon a surface per unit area. The unit of irradiance is (W/m^2) [9]. Note that the irradiance on a surface is dependent on both the area of the surface being illuminated and the angle of that surface relative to the source of the light.

2.3.3 Spectral Quantities

When evaluating spectral quantities, it is necessary to consider how different objects or surfaces respond to various frequencies of light. As such, all of the listed quantities are given as a function of wavelength, λ . Spectral quantities are denoted by including the term "spectral" in the name, and by a subscript λ (e.g., Φ_λ and E_λ).

2.3.3.1 Relevant Spectral Terms

Monochromatic Radiation: Light consisting of just a single wavelength. Example: laser

Near Monochromatic Radiation: Light consisting of a narrow group of wavelengths. Example: light-emitting diodes and band pass filtered sources

Continuous Spectra Radiation: Light consisting of a relatively wide range of wavelengths with no gaps. Example: incandescent bulbs

Band Spectra Radiation: Light consisting of multiple frequencies, but with gaps separating the individual regions of radiation. Example: gaseous discharge lamps, such as helium or xenon lamps

Spectral Radiant Power $\Phi_\lambda(\lambda)$: defined as a source's radiant power per wavelength interval as a function of wavelength. The unit of spectral radiant power is (W/nm) or (W/Å)

Spectral Irradiance E_λ : The amount of radiant power impinging upon a surface per unit area, as a function of wavelength. The unit¹ of irradiance is ((W/m²)/nm) or ((W/m²)/Å) [9].

2.3.4 Photometric Quantities

Photometric quantities are denoted by including the term "luminous" in the name, and by a subscript v , for "visual" (e.g., Φ_v and E_v). These quantities represent similar values to their radiometric counterparts, except that instead of being a direct sum of power across the light spectrum, they represent a weighted sum of the power where each value at a given frequency has been scaled according to how responsive the human eye is to light at that frequency. In addition, there are separate scaling functions depending on the light level in question.

2.3.4.1 Relevant Photometric Terms

Photopic Vision: The human eye's sensitivity under daylight conditions. Photopic vision takes place when the eye is adapted to luminance levels of at least several candelas per square meters.

Scotopic Vision: The human eye's sensitivity under low-light conditions. Scotopic vision takes place when the eye is adapted to luminance levels below some hundredths of a candela per square meter.

Photometric quantities relating to scotopic vision are denoted by an additional prime, for example Φ_v'

Spectral luminous efficiency function $V(\lambda)$: The spectral sensitivity function of the average human eye under daylight conditions (photopic vision) [9].

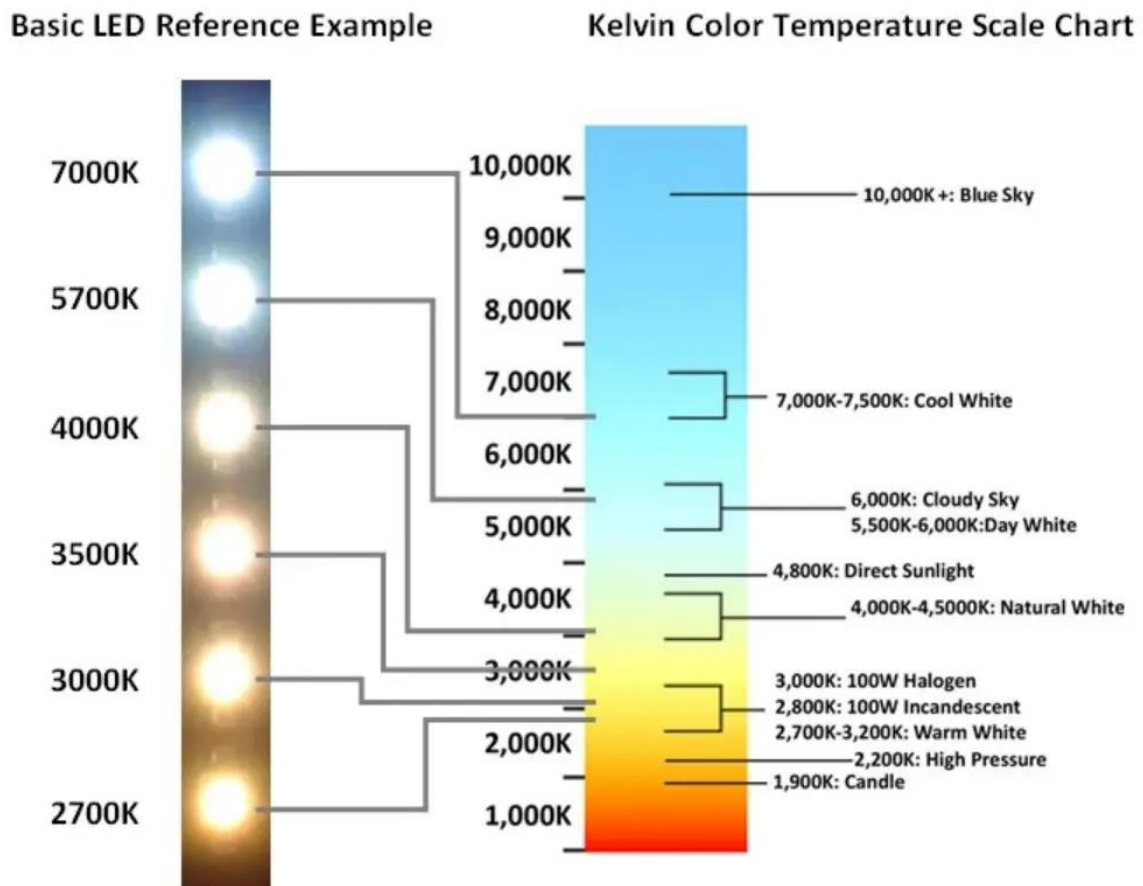
¹ Technically this could be reduced to GW/m³ or W/mm³, but neither of those are particularly helpful units in the given context

Luminous Flux Φ_v : The basic photometric quantity and describes the total amount of electromagnetic radiation emitted by a source, spectrally weighted with the human eye's spectral luminous efficiency function, $V(\lambda)$. Luminous flux is the photometric counterpart to radiant power. The unit of luminous flux is lumen (lm) [9].

Illuminance E_v : The luminous flux per area impinging upon a certain location of an irradiated surface. The unit of illuminance is lux (lx), and $1 \text{ lx} = 1 \text{ lm/m}^2$ [9].

Color Temperature: A way of expressing the spectral distribution of a light source as a single value. As explained by an online tutorial by Gigahertz-Optic, "The color temperature is given in Kelvin (K) and is the temperature of the blackbody (Planckian) radiator whose received color most closely resembles that of a given color stimulus" [9]. Figure 5 shows an example of different color temperatures and how they related to the perceived color and "warmth" of an LED bulb.

Figure 5: Light Bulb Color Temperature Chart [10]



2.3.5 Converting From Radiometric Quantities to Spectral or Photometric Quantities

Reference [9] provides the following descriptions for how to convert from radiometric values to other quantities.

2.3.5.1 Monochromatic Radiation:

In the case of monochromatic radiation at a certain wavelength, λ , a radiometric quantity, X_e , is simply transformed to its photometric counterpart, X_v , by multiplication with the respective spectral luminous efficiency, $V(\lambda)$, and by the factor

$$K_m := 683 \frac{\text{lm}}{\text{W}}$$

Thus,

$$X_v = X_e \cdot V(\lambda) \cdot 683 \cdot \frac{\text{lm}}{\text{W}}$$

with X denoting one of the quantities such as Φ or E.

2.3.5.2 Polychromatic Radiation

If a source emits polychromatic light described by the spectral radiant power, $\Phi_\lambda(\lambda)$, its luminous flux can be calculated by spectral weighting of $\Phi_\lambda(\lambda)$ with the human eye's spectral luminous efficiency function, $V(\lambda)$, integration over wavelength and multiplication with $K_m = 683 \text{ lm/W}$, so:

$$\Phi_v = K_m \cdot \Phi_\lambda(\lambda) \cdot V(\lambda) d\lambda$$

In general, a photometric quantity, X_v , is calculated from its spectral radiometric counterpart, $X_\lambda(\lambda)$, by the relation:

$$X_v = K_m(\lambda) \cdot V(\lambda) d\lambda$$

with X denoting one of the quantities such as Φ , or E.

2.3.6 Summary Of Quantities and Units

Figure 6 and Figure 7 from Gigahertz-Optik provide a summary of the different quantities associated with light measurement, as well as their respective units.

Figure 6: Gigahertz-Optik Table of Fundamental Units, Part 1. [9]

VII.1. Relevant quantities, their symbols and units		
Quantity	Symbol	Unit(s)
Wavelength	λ	1 nanometer = 1 nm = 10^{-9} m / 1 Ångström = 1 Å = 10^{-10} m
Power	P	1 Watt = 1 W
Solid angle	Ω	1 steradian = 1 sr
Radiant power or radiant flux	Φ_e	1 Watt = 1 W
Radiant intensity	I_e	1 W sr ⁻¹
Radiance	L_e	1 W sr ⁻¹ m ⁻²
Irradiance	E_e	1 W m ⁻²
Radiant exitance	M_e	1 W m ⁻²
Luminous flux	Φ_v	1 lumen = 1 lm photopic: 1 lm corresponds to $\Phi_e = 1/683$ W at $\lambda_m = 555$ nm scotopic: 1 lm corresponds to $\Phi_e = 1/1700$ W at $\lambda'_m = 507$ nm
Luminous intensity	I_v	1 candela = 1 cd = 1 lm / sr
Luminance	L_v	1 lm sr ⁻¹ m ⁻² = 1 cd m ⁻² = 1 nit 1 stilb = 1 sb = 1 cd m ⁻² 1 apostilb = 1 asb = $1/\pi$ cd m ⁻² 1 lambert = 1 L = $10^4/\pi$ cd m ⁻² 1 footlambert = 1 fl = 3.426 cd m ⁻²
Illuminance	E_v	1 lux = 1 lx = 1 lm m ⁻² 1 phot = 1 ph = 10^4 lx 1 footcandle = 1 fc = 1 lm ft ⁻² = 10.764 lx

Figure 7: Gigahertz-Optik Table of Fundamental Units, Part 2 [9]

Page 194 - Tutorials



Appendix

Quantity	Symbol	Unit(s)
Luminous exitance	M_v	1 lm m ⁻²
Spectral radiant power	$\Phi_{e,\lambda}$	1 W nm ⁻¹
Spectral radiant intensity	$I_{e,\lambda}$	1 W sr ⁻¹ nm ⁻¹
Spectral radiance	$L_{e,\lambda}$	1 W sr ⁻¹ m ⁻² nm ⁻¹
Spectral irradiance	$E_{e,\lambda}$	1 W m ⁻² nm ⁻¹
Spectral radiant exitance	$M_{e,\lambda}$	1 W m ⁻² nm ⁻¹

Table VII.IV. *Units in italic are not SI units, not consistent with CIE regulations and should not be used!*

VII.2. Summary of radiometric and photometric quantities				
Quantification of electromagnetic radiation ...	Radiometric quantity	Spectral quantity	Photometric quantity	quantity depends on
... emitted by a source in total	radiant power Φ_e W	spectral radiant power $\Phi_{e,\lambda}$ W nm ⁻¹	luminous flux Φ_v lm (lumen)	-
... emitted in a certain direction	radiant intensity I_e W sr ⁻¹	spectral radiant intensity $I_{e,\lambda}$ W sr ⁻¹ nm ⁻¹	luminous intensity I_v lm / sr = cd	direction
... emitted by a location on a surface	radiant exitance M_e W m ⁻²	spectral radiant exitance $M_{e,\lambda}$ W m ⁻² nm ⁻¹	luminous exitance M_v lm m ⁻²	position on source's surface
... emitted by a location on a surface in a certain direction	radiance L_e W sr ⁻¹ m ⁻²	spectral radiance $L_{e,\lambda}$ W sr ⁻¹ m ⁻² nm ⁻¹	luminance L_v lm sr ⁻¹ m ⁻² = cd m ⁻²	position on source's surface and direction
... impinging upon a surface	irradiance E_e W m ⁻²	spectral irradiance $E_{e,\lambda}$ W m ⁻² nm ⁻¹	illuminance E_v lm m ⁻² = lx	position on irradiated surface

Table VII.V – Radiometric and photometric quantities

2.3.7 Relevance to Flicker Research

Obviously, to be able to reliably quantify flicker characteristics, it is crucial to have an understanding of what, exactly, is being measured. All the direct measurements and outputs for the test fixture were in terms of volts and amperes. Unfortunately, residential and commercial light bulbs do not typically list their radiometric quantities or emission spectra. Instead, the consumer is typically given a value in lumens and a "Color Temperature" in degrees Kelvin. While these values are generally enough for a consumer—personal experience indicates most people base their purchasing decisions on the listed watt equivalent and the description of "soft white", "daylight", etc.—they do not provide sufficient information for spectral or radiometric analysis. In addition, the spectral response of a given bulb can actually change, depending on the age of the bulb [11]. Some examples of the variation in spectral response for various bulbs is given in Figure 8:

Figure 8: Spectral Response of Several Different Kinds of Light Bulbs [12]

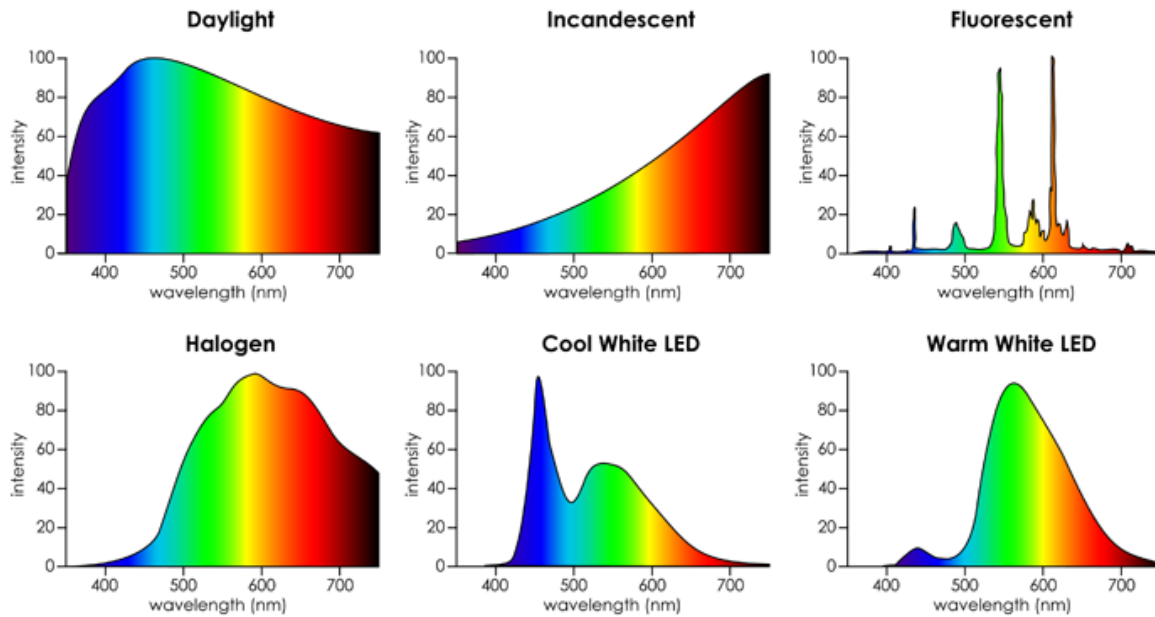


Table 1 denotes the units and quantities involved in each step of the signal generation, capture, and recording process for this research.

Table 1: Applicable Units at Different Stages in the Test Sequence

Stage	Applicable Units
Generated Signal (V_{gen})	Volts (V)
Amplified Signal (V_{bulb} and C_{bulb})	Volts (V), Amperes (A)
Light output from bulb (Luminous flux)	Lumens (lm), Color Temperature (K)
Energy incident on light sensor input (irradiance)	Watts Per Square Meter (W/m^2)
Light sensor measurements (power)	Watts (W), Aperture Area (m^2)
Light sensor output	Volts (V)

Section 5.2 of this thesis discusses the specifics of how, for this research, it was possible to abstract the above steps and treat the test system as a Voltage Signal in \rightarrow Measured Voltage Out. This abstraction would not have been possible to do with confidence without understanding the quantities and units involved.

2.4 Flicker Background

2.4.1 Introduction To Flicker

Light flicker has long been an issue on the power system and is associated with a number of health-related issues, including epileptic seizures and headaches/migraines [13]. Attempts to classify and understand electrically caused light flicker were occurring as far back as 1926 [14]. In the 1950s, Westinghouse published guides on the causes of light flicker, as well as mitigation techniques [15]. The increasing popularity of LED light bulbs in recent years is creating new challenges in terms of the measurement, classification, and mitigation of light flicker, as well as revealing deficiencies in previously defined measurement tools. This section provides an overview of health risks associated with light flicker; a list of some of the common sources of flicker on the power system; several methods of measuring and classifying flicker, particularly in relation to LED light bulbs; and other findings related to LED light flicker.

2.4.2 Terms Associated with Light Flicker

The following section defines several terms that commonly appear in the literature associated with flicker research.

Flicker: “Variations in luminance over time” [13]. Although some sources use a more restrictive definition that implies that the fluctuation is directly visible or else repetitive, for the purposes of this paper we will use the broader definition.

Critical Flicker Fusion (CFF) Frequency: The maximum frequency at which flicker is visible to an observer. This is generally determined to be in the range of 60–100 Hz, though sources cite slightly different numbers [13] [16] [17].

Interharmonics: “Non-integer multiples of the fundamental frequency” [18] (i.e. anything other than 60 Hz, 120 Hz, 240 Hz, etc. on a 60 Hz system or 50 Hz, 100 Hz, 150 Hz, etc. on a 50 Hz system).

2.4.3 Negative Effects of Flicker

The range of frequencies for which flicker is observable varies depending upon lighting conditions as well as on the observer. While the CFF frequency is typically listed as being in the 60–100 Hz range, the most noticeable frequencies tend to be in the narrower 6–12 Hz range [15]. The health effects related to flicker do not stop at the CFF frequency, though, and some the more commonly mentioned issues are listed below.

2.4.3.1 *Epileptic Seizures:*

There are a number of health-related issues that have been attributed to light flicker, one of the most extreme examples being photosensitive epileptic seizures. For a certain small percentage of the population, lights flickering with sufficient amplitude in a particular frequency range can induce an epileptic seizure. The exact intensity and frequency that presents the highest risk varies from person to person, but anything within the range of 3 Hz–70 Hz presents a risk, with the most troublesome region being between 15 Hz–25 Hz [13] [19].

2.4.3.2 *Stroboscopic Effect:*

Another potentially catastrophic effect related to light flicker is caused by the stroboscopic effect. This is where intermittent lighting can cause objects to appear to be moving at a different speed than they actually are. The main risk associated with the stroboscopic effect is that it can cause moving or rotating machinery to appear to be moving much slower than in reality, or even not moving at all. This presents the risk of someone accidentally touching a moving piece of equipment under the impression that it is actually not moving at all. Studies have indicated that stroboscopic effects may

be visible at frequencies as high as several thousand hertz [19] [20]. Similar frequency ranges were reported for a related effect known as intrasaccadic images, which is where rapid eye movements (saccades) in the presence of a flickering light produces the illusion of a series of discrete, independent images. These can appear as a trail of light images when viewed under certain circumstances, such as being behind a vehicle with LED taillights [19].

2.4.3.3 Migraines and Headaches:

Another effect of light flicker is an increase in the number migraines and headaches experienced by people exposed to the flicker. Lehman and Wilkins [19] cite an example of the average number of headaches doubling for office workers exposed to flickering caused by conventional magnetic ballasts in fluorescent light fixtures. An interesting side note from this paper is that the doubling in headaches was due less to an increase in the number of people getting headaches but rather to a small percentage of the population getting much more frequent headaches.

2.4.4 Sources of Flicker

In order to try to mitigate flicker on lighting systems, it is important to understand what is causing the flicker. The nature of the flicker source has a drastic effect on the type of flicker that is produced. Additionally, certain types of LED lighting are susceptible to flicker in ways that conventional incandescent lights are not, as will be shown later in this paper. Some of the more common sources of LED light flicker are given below.

Large loads/current draw: One of the biggest causes of flicker across all forms of lighting is the starting and stopping of large/high current loads. Anything capable of causing sudden changes on the power system can be considered as a source of flicker. Griscom [15] goes into extensive detail about some of the common sources of large voltage variation on the power system, the nature of the variation, and possible mitigation techniques. The provided examples include irregularities in generation, short circuits/faults/switching surges, motor starting, motor-driven reciprocating loads (pumps, compressors, etc.), electric smelting furnaces, electric welders, and large industrial processes (metal stamps, rolling mills, strip miners). Some of the information in that book chapter is outdated—the outright dismissal of voltage regulators for controlling flicker is one good example, when modern power electronics are used for exactly that purpose. However, the majority of the content is still very relevant to flicker control. The main suggestions for controlling voltage fluctuations include motor-generator sets with flywheels to suppress transients, soft-starting large motors to reduce current draw, using synchronous condensers to alter system impedance, and

strengthening the system (adding more supply capability) in areas where other options are not practical. All the listed options are commonly used today.

Power system communications: The faster response time of LED lights, as compared to incandescent bulbs, makes some designs susceptible to flicker from common power line communication (also called power line carrier or PLC) techniques. An example of this is given in the article by Rahman, Elphick, Muttaqi, and David [21]. In this case, they were evaluating the effect of a type of PLC called audio frequency injection control (AFIC) on various forms of LED lights. This investigation was sparked by a number of customer complaints of flicker on LED lighting systems with dimmers. The study determined that AFIC signals did indeed cause observable and potentially disruptive levels of flicker for certain LED light bulb and dimmer combinations. While this study is just a single example, it does show that PLC techniques can produce observable flicker with LED light bulbs.

Switching power supplies/interharmonics: Switching power supplies represent an increasingly common source of LED flicker. In addition to causing voltage variations directly at their frequency of operation, these power supplies can induce additional forms of flicker if they are operated at interharmonics near (but not quite at) the harmonic frequencies of the fundamental power system. These induced flickers can appear at frequencies much lower than either the power system fundamental frequency or the power supply switching frequency. For example; Kim, Rylander, Powers, Grady, and Arapostathis [18] showed that it is possible to generate an 8 Hz flicker on LED lamps by injecting 0.5% interharmonics at frequencies $180 + 8$ Hz or $300 + 8$ Hz.

Variable frequency drives: Variable frequency drives (VFDs) present yet another potential source of flicker on top of those already established. In addition to having the switching power supply characteristics described above, VFDs have the additional challenge of ripple frequencies leaking through from one side of the device to the other. The example given by Virulkar and Aware [22] is of a VFD powered by 60 Hz driving a motor output at 50 Hz. This will result in the DC link on the device having both 50 Hz and 60 Hz ripple. Depending on the design of the drive, it may be possible for the 50 Hz component to then be injected onto the power system, resulting in the type of interharmonic behaviors described above.

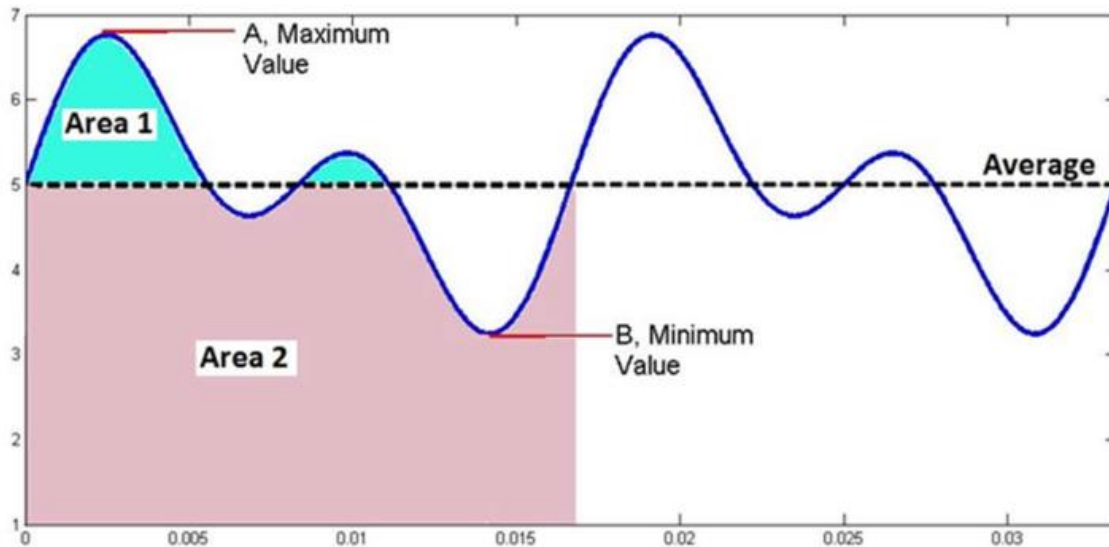
2.4.5 Flicker Classifications

The traditional method for measuring and quantifying light flicker has been through the use of a flickermeter, as described by IEC 61000-4-15 [13] [23]. This method involves modeling the perceived flicker of a light source by measuring the voltage input of the light source and passing it through a series of filters designed to simulate the “lamp-eye-brain” response of the human body [5]

[24]. The problem with this design is that the filters were originally designed based on the flicker behavior of conventional incandescent lights and do not model higher frequency effects or interharmonics [18].

Two of the main metrics for evaluating light flicker are given below. Both of these metrics are based on the relative illuminance of a source over time, as shown in Figure 9.

Figure 9: Flicker Classifications [13]



2.4.5.1 Percent Flicker

$$\% \text{ Flicker} = \frac{\text{Max} - \text{Min}}{\text{Max} + \text{Min}} \cdot 100$$

This metric, also called peak-to-peak contrast, Michelson contrast, or Modulation (%) [13], gives a scaled reference for the absolute maximum and minimum present in the light output. Despite being one of the most frequently used flicker metrics present in the reviewed literature, it has some notable inadequacies. The first inadequacy is that it does not take into account the actual shape of the waveform. By only looking at the extremes, this metric may gloss over other aspects of the light output that could contribute to flicker. The other issue with percent flicker as a metric is that, in this form, it does not take into account the frequency of the flicker. It is possible to have light output with 100% modulation with no noticeable problems, provided that the frequency of modulation is high enough [16] [21]. An example of this effect occurs with dimmers that operate by using high frequency pulse width modulation (PWM).

2.4.5.2 *Flicker Index*

$$\text{Flicker Index} = \frac{\text{Area}_1}{\text{Area}_1 + \text{Area}_2}$$

The flicker index of a light compares the area of a light output curve that is above the average to the total area of the curve for a single cycle. This gives a more accurate representation than percent flicker because, by integrating the total light output over a cycle and comparing the above average portion to the total output, it accounts for any distortion that may be present in the waveform [25]. However, like percent flicker, the flicker index still does not take into account the frequency of the flicker. This means that a light source could have a comparatively high flicker index but still be operating at a high-enough frequency that it does not present any noticeable effects [21].

2.4.5.3 *IEEE Flicker Guidance*

In order to address the frequency limitations of flicker index and percent flicker, the IEEE has issued guidance relating maximum acceptable flicker percentage—listed in the guidance text as Modulation (%)—for various frequency ranges. As the frequency increases, so does the acceptable flicker percentage [13].

There are three different recommended practices presented in the IEEE standard: the choice of which practice to apply depends on the application and what types of risk the system or bulb designer wants to mitigate. The recommendations can overlap, and the system can adhere to more than one of the recommendations, as long as the more restrictive set of values are chosen for a given frequency range.

Recommended Practice 1: "If it is desired to limit possible adverse biological effects of flicker"

$$\text{Max}_{\%}(f) = \begin{cases} 0.2\% & \text{if } f < 8\text{Hz} \\ 0.025f\% & \text{if } 8\text{Hz} \leq f < 90\text{Hz} \\ .08f\% & \text{if } 90\text{Hz} \leq f < 1250\text{Hz} \\ \text{Unrestricted (100\%)} & \text{if } 1250\text{Hz} \leq f \end{cases}$$

This practice is designed to limit negative physical effects such as migraines and seizures, but may still allow for some observable flicker effect, such as the stroboscopic effect and observable flicker during eye saccades. This is a "middle ground" practice and is what is given as the primary recommendation in the standard.

Recommended Practice 2: "If it is desired to operate within the recommended 'No Observable Effect Level' (NOEL) of flicker"

$$\text{Max}_{\%}(f) = \begin{cases} 0.08\% & \text{if } f < 8\text{Hz} \\ (0.01f)\% & \text{if } 8\text{Hz} \leq f < 90\text{Hz} \\ (.0333f)\% & \text{if } 90\text{Hz} \leq f < 3000\text{Hz} \\ \text{Unrestricted (100\%)} & \text{if } 3000\text{Hz} \leq f \end{cases}$$

This practice is designed to be the most restrictive case, with the intent being to eliminate all observable effects of flicker. It is achieved by reducing the allowable level of flicker from Practice 1 by 2.5x and by extending the maximum controlled frequency range from 1250 Hz out to 3000 Hz.

Recommended Practice 3: "For seizure prevention, applies to any lighting source, under all operating scenarios"

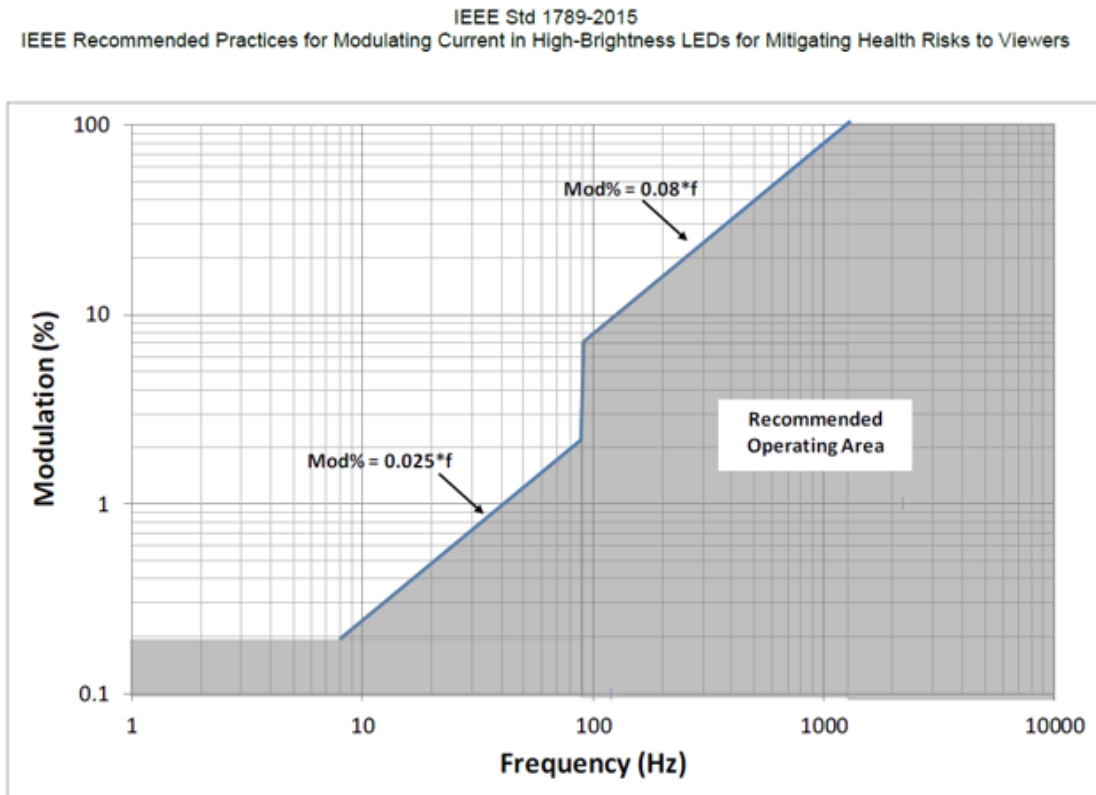
$$\text{Max}_{\%}(f) = \begin{cases} 5\% & \text{if } f < 90\text{Hz} \\ \text{Unrestricted (100\%)} & \text{if } 90\text{Hz} \leq f \end{cases}$$

This is the least restrictive of the recommended practices as it is only concerned with seizure prevention, not any other biological effects. This recommendation simply states that under any conditions all flicker with a frequency below 90 Hz must be limited to 5% modulation or less.

However, despite it being the least restrictive in terms of allowable frequencies and percent flicker, it is the only one that is not considered optional. Practice 1 and Practice 2 can be implemented or not depending on if it is desired to limit a certain level of effect, but Practice 3 deals with a safety-critical issue and should always be followed.

Figure 10 gives an example of the ranges and values for recommended Practice 1.

Figure 10: IEEE Flicker Guidelines [13]



NOTE—Operating in the shaded area minimizes visual discomfort or annoyance and also gives low risk for headaches and photosensitive epileptic seizures. Below 90 Hz, Modulation (%) is less than $0.025 \times \text{frequency}$. At or above 90 Hz, Modulation (%) is below $0.08 \times \text{frequency}$. Modulation (%) = $100 \times (L_{max} - L_{min}) / (L_{max} + L_{min})$ where L_{max} and L_{min} correspond to the maximum and minimum luminance, respectively. The figure was derived from the low-risk regions in Figure 18.

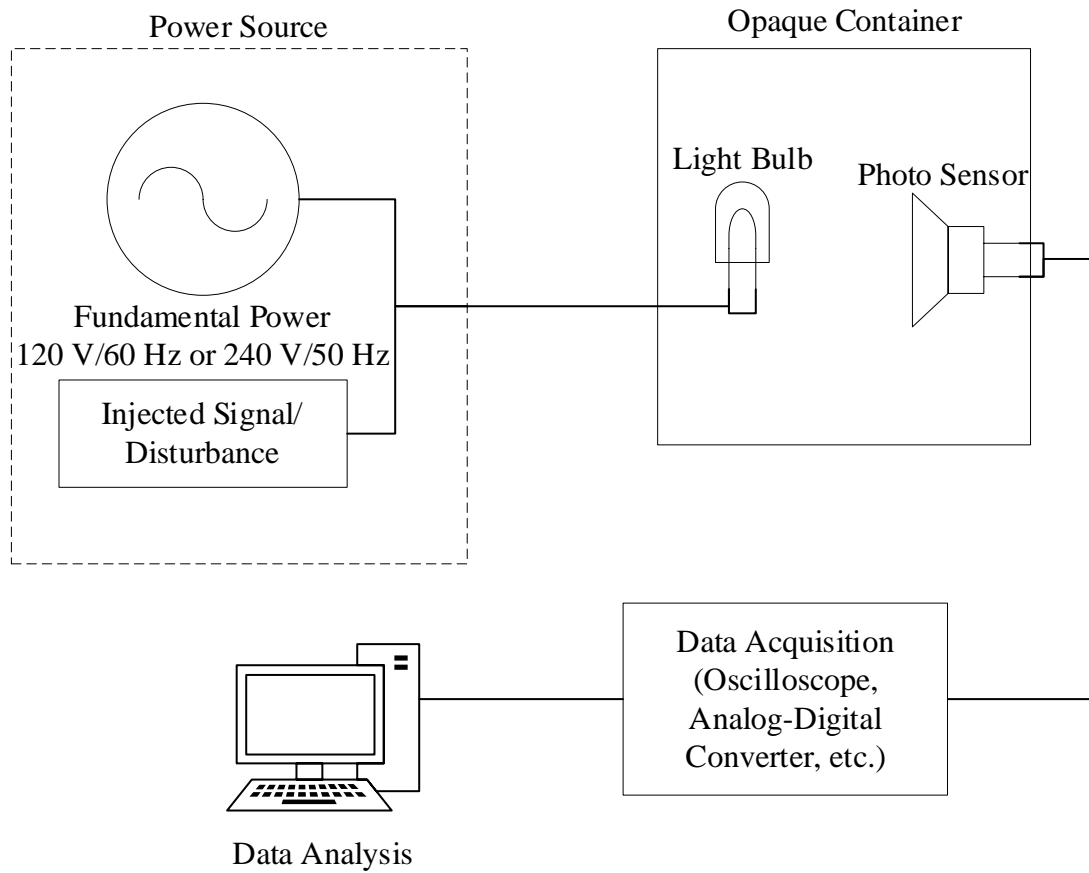
2.5 Previous Research

2.5.1 Common Test Setup Configuration

In recent years, a number of studies have been conducted to analyze the flicker output of LED light bulbs in response to various stimuli. Though the specifics varied in terms of the equipment used and the effects studied, all the studies had the same basic setup. This consisted of a power supply, some method of injecting noise/disturbances, an opaque enclosure containing the light bulb under test and a photo sensor, a device for capturing the output from the light sensor, and a PC for data processing.

An approximation of the common test setup is shown in Figure 11.

Figure 11: Generic Light Flicker Test Setup



The setups for each of the reviewed studies are summarized in Table 2.

Table 2: Summary of prior research

Author(s)	Attribute of interest	Comment
Lehman, Wilkins, Berman, Poplawski, Miller [16]	Developing a method of classifying low frequency flicker using truncated Fourier series approximation	Test results clearly demonstrate the wide range of LED flicker responses
Kobav [17]	Characterizing flicker response of a variety of light bulbs, including incandescent, halogen, fluorescent, and LED	Test setup was unique in that there were two light boxes, each with one side open. Inducing flicker on one bulb but not the other allowed for side-by-side visual comparison
Kim, Rylander, Powers, Grady, Arapostathis [18]	Studying the effect of interharmonics on light bulb flicker	Report demonstrated ability of interharmonics to create flicker effects at frequencies well below the fundamental
Rahman, Elphick, Muttaqi, David [21]	Measured the effects of audio frequency injection control (AFIC) on LED light output in the presence of dimmer switches	Showed that certain LED designs are susceptible to flicker caused by PLC type controls, particularly when used with dimmer switches
Cai, Cobben, Myrzik, Blom, Kling [5]	Comparing results from IEC 61000-4-15 flicker meter to those of a photo sensor setup for various bulbs at different frequencies (DC-25 Hz).	Scaled test by making light outputs match and then measuring voltage characteristics
Drapela, Langella, Testa, Collin, Xu, Djokic [26]	Attempted to classify the light vs modulation input frequency response for several different styles of LED driving circuit	Test cases were specifically chosen to cover different LED bulb circuit topologies, which has the effect of ranking LED bulb styles by which ones are most prone to flicker
Chmielowiec [7]	Survey of flicker response for various types of light bulbs in the range of DC-25 Hz	Results very similar to other studies
Drapela, Slezingr [24]	Also attempting to develop an alternative to the IEC 61000-4-15 flicker meter	Results very similar to those of Cai et al., but with much wider frequency ranges
Sakar, Rönnerberg, Bollen [27]	Applying standard IEC test profiles to LED light bulbs	Encountered effects like those seen by Kim et al. where interharmonics were able to cause flicker at frequencies well below the fundamental frequency

2.5.2 Generalized Findings

The overall observed trend for these results is that it is very difficult to consistently categorize what types of disturbances will or will not cause flicker with an LED light bulb. The wide range of driver characteristics for different bulbs means that a variety of inputs can cause flicker on a specific LED bulb, but very few things will cause it for all types of bulbs. The research of Drapela et al. [5] provides a good example of just how much variation can be found in LED light bulb behavior, as shown in Figure 12.

Figure 12: Example of Circuit Topology and Flicker Response of Two Different LED Drivers [26]

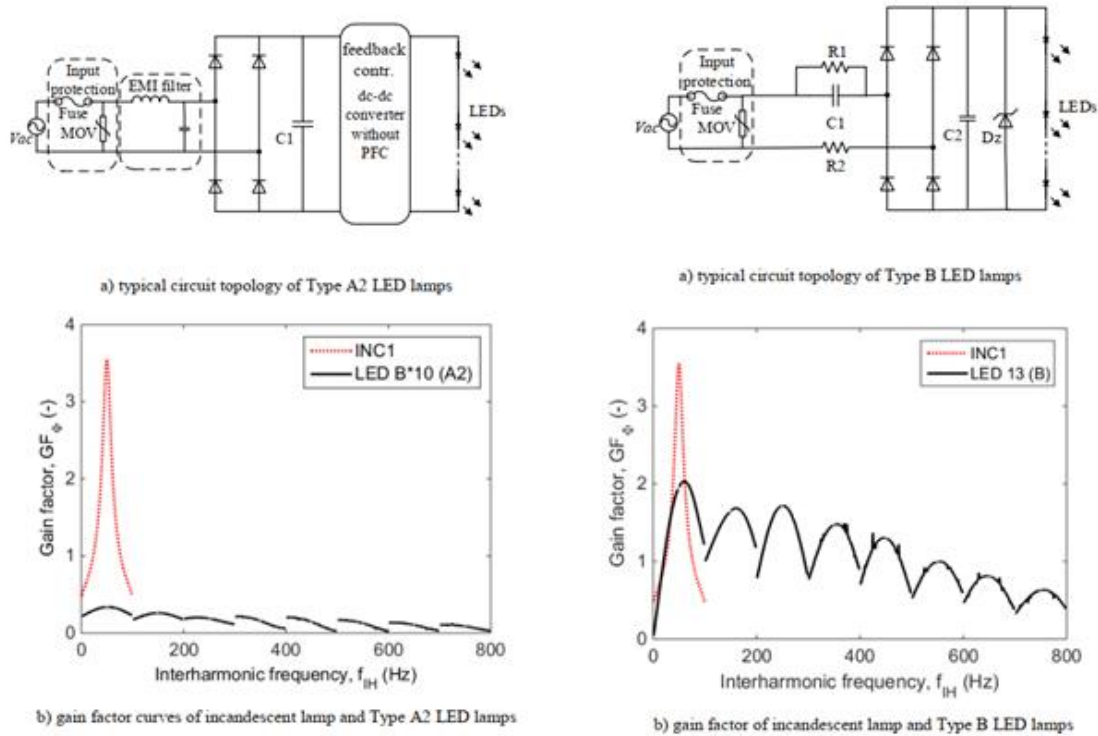
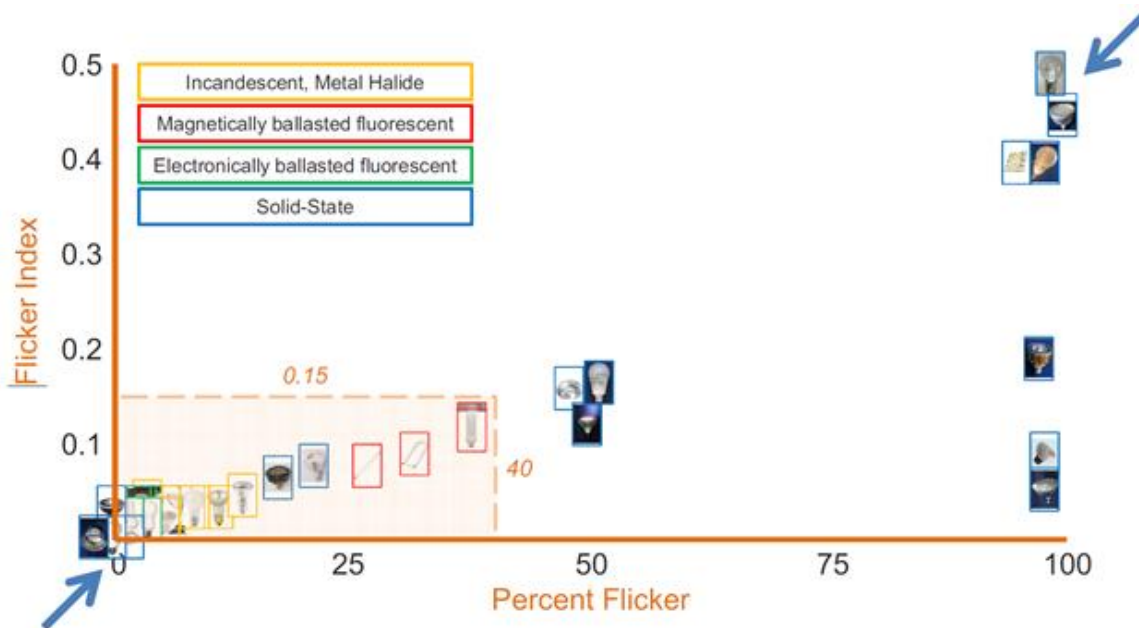


Figure 12 shows the driver circuits for two different kinds of LED light bulbs, as well as their associated gain factors—which can be thought of as a measure of how sensitive the light output of the bulb is to input voltage variations. While both circuits convert the input AC voltage to a DC value in order to drive the output LEDs, the circuit on the left features electromagnetic interference (EMI) filtering on the input and dedicated output voltage regulation. By contrast, the circuit on the right actually passes high frequency noise, instead of attenuating it, and does very little to control the output voltage, aside from limiting how high said voltage can go through the use of a Zener diode.

The gain factor graphs demonstrate just how much of an effect the support circuitry has on the bulb's sensitivity to input voltage disruptions, especially considering that the authors of the study had to multiply the plot for the type A2 LED lamp by a factor of 10 just to make it visible relative to the incandescent bulb. The red line in both graphs is the gain factor of a traditional incandescent light bulb, plotted for reference.

The wide variation in flicker sensitivity among LED light bulbs is shown very well by the final figure in the report from Lehman et al. [16], which is given in Figure 13.

Figure 13: Examples of Flicker Response for Various Types of Bulbs [16]



2.5.3 Summary Of Previous Research

The research into the effects of light flicker on humans is extensive and ongoing, as is the research into the types of events that are prone to cause light flicker. While measurement standards and metrics have been established for evaluating flicker, they are often insufficient when dealing with the types of flicker produced by LED light bulbs. The wide variety of designs and driver circuits present in LED bulbs makes it difficult to establish a generic flicker behavior model.

While most researchers employed similar designs for their test setups, the specific attributes studied varied from paper to paper. Some papers focused only on low frequency tests, while others focused on interharmonic behaviors or the effects of a specific input type. One aspect that was not covered in the reviewed literature was the wide-spectrum frequency response of the light bulbs in question.

Typically, the studies picked a few frequencies of interest or else did a sweep within a narrow band of frequencies. A full sweep of the input frequencies for an LED bulb, from DC to the limit of stroboscopic effect detection, may provide valuable insight into what frequencies are likely to cause the worst flicker as well as help quantify the effects caused by interharmonic noise. Additionally, most of the studies only analyzed the low frequency response of conventional incandescent bulbs or else just accepted the given model as being accurate. Another possible avenue of research would be to analyze the higher frequency behaviors of incandescent bulbs using a photo sensor setup such as was described in Figure 11 to determine if the accepted models are indeed accurate.

As the popularity of LED bulbs for commercial and residential lighting continues to grow, the need to understand, quantify, and control the flicker generated by these lights will continue to grow as well. Having an understanding of the sources of flicker, the types of effects flicker might cause, and what techniques can be used to mitigate flicker may have a crucial effect on enhancing safety, comfort, and productivity in both the home and the workplace.

2.6 Background Summary

Section 2.1 provided a brief overview of the types of bulbs being evaluated in this research, as well as a high-level overview of their principles of operation. The information provided in Section 2.3 provides a knowledge base for understanding what quantities need to be measured, how to measure and evaluate those quantities, and the relationships between the various quantities. Section 2.4 provided an overview of negative health effects of light flicker, sources of flicker, and ways of classifying flicker behavior. Section 2.5 provided an overview of the previous research that has been done on flicker characteristics, a sample generalized test setup, and examples of other researcher's results and findings. These sections provide a foundation for the development of a testbed and toolchain to study and analyze flicker behavior.

Chapter 3: Test Setup

3.1 Introduction

As mentioned in Section 2.5.1, most if not all test setups for observing and measuring light flicker consist of a power supply, some method of injecting noise/disturbances, an opaque enclosure containing both the light bulb under test and a photo sensor, a device for capturing the output from the light sensor, and a PC for data processing. The test setup for this research was no exception to that general layout. In this case, however, there is an additional focus on being able to capture higher frequency behavior than is typically monitored in flicker studies. There is also a focus on trying to make a direct comparison between the inputs to the bulb (voltage and current) and recorded outputs from the bulb (relative light output). This focus on having higher frequency captures with multiple quantities drove many of the design decisions for the testbed and ultimately proved much harder to implement than initially expected. This chapter covers the physical hardware and overall equipment design developed for this research, as well as the basic sequence for performing flicker/light output tests. Chapter 4 covers the procedure and tools that were developed to actually accomplish the tests with the desired timing, sequencing, and resolution.

3.2 National Instruments Data Acquisition Platform

Possibly the most critical component of the entire test setup is the National Instruments (NI) data acquisition (DAQ) platform. It plays a central role in both the generation and capture of data. The majority of the time and effort for this project was spent on developing code to interface with the DAQ devices. Getting the DAQ code base working served as the catalyst for creating the entire H5 toolchain (see Chapter 4). Because the DAQ platform is so central to the entire test structure, some additional explanation and description is warranted.

3.2.1 What Is a DAQ?

When referred to verbally, the term DAQ can sound confusingly close to the acronym DAC, which stands for “digital to analog converter.” This potential confusion is compounded by the fact that one of the main use cases for this NI product line is generating analog signals from digital data, which is to say a DAQ can be used as a DAC. Some clarification of terms is provided below:

DAQ: In this context DAQ stands for “**Data AcQ**uisition,” a series of devices sold by National Instruments that is designed specifically to provide robust, high-speed, high-resolution data generation and capture with a programmable interface [28]. The DAQ² product line is designed to support input and output of digital, analog, and counter values.

DAC: This is an acronym for “digital to analog converter” which is a device designed to take digital data and output it as analog values, such as voltage or current.

ADC: This is an acronym for “analog to digital converter” which is a device designed to receive analog values, such as voltage, and quantize it into discrete values that can be represented digitally.

The analog input and output devices used for this experiment all support four or more channels of ± 10 V data, each with 16-bit resolution and sample rates of 100K samples/second. A typical DAQ setup involves a chassis, one or more modules or “cards,” and some sort of controller. Anecdotally, the naming convention used by NI for when these devices are separate versus when they are combined has caused significant confusion when trying to explain the interactions and functioning of said devices; see Section 3.2.2 for a more detailed description of the individual components of a DAQ setup.

3.2.2 DAQ Components

As mentioned in Section 3.2, the NI DAQ series of devices were chosen for the signal generation and data capture components of this project. Their combination of high sample rate, good resolution, and comparatively low price—at least compared to other lab-grade equipment—made them a good choice for this project. In addition, several other projects were already making use of the platform, and some preliminary data generation and capture tools had already been created.

As mentioned above, there is potential for confusion regarding the naming convention implemented by NI for the DAQ equipment. The following sections offer a brief description of the individual components and are intended to help resolve the potential naming confusion.

² Technically the line of products used for this research is part of the compact DAQ or “cDAQ” subset of the wider DAQ product line, but the distinction is of limited relevance to this report and has been omitted.

3.2.2.1 Chassis:

The DAQ chassis is the base unit for using the DAQ platform. It consists of an aluminum housing and one or more slots where individual modules can be connected. The chassis is also the part that connects directly to the computer or whatever device is providing the control logic. Most often the connection is via USB, though other options, such as ethernet, are available. Figure 14 shows an example of a chassis with multiple slots and one with just a single slot.

Figure 14: Example of a Single-Slot vs. Multi-Slot DAQ Chassis [28]



3.2.2.2 Module:

A module, or “card,” is the part of the DAQ setup that handles the actual data generation or capture. The modules are individual devices that mount into one of the slots on a DAQ chassis and can be swapped in and out, depending on the specific requirements of the research. As of the time of this writing, there are over sixty different module variants available from NI. Figure 15 shows some examples of the different kinds of modules available. This research made use of an NI-9263 C Series [29] Voltage Output Module and an NI-9215 C Series Voltage Input Module [30]. The chassis used for testing was a cDAQ-9174 NI CompactDAQ Chassis [31].

Though there were a number of available input and output voltage modules that would have met the testing requirements, the listed modules were chosen largely due to their terminal configuration and channel count. Specifically they both have screw-type terminals, which were found to provide a more reliable connection than the spring-type terminals that were also available. In addition, both modules had four available channels, which was sufficient for testing without having an abundance of unused channels.

Figure 15: Example of Some of the Module Options Available [28]



3.2.2.3 *Device*

There is some ambiguity as to what the NI documentation means when it refers to something as a “device.” This is especially prominent when interacting with the application programming interface (API)³ where, depending on context, the term device may refer to the chassis, the module, or the combination of a chassis and one or more modules. To minimize confusion, the terms “module” and “chassis” will be favored over the term “device” in contexts where the distinction is important.

3.2.2.4 *Channel*

Each of the modules features one or more data channels. This is the individual physical connection to some external element, such as a sensor or amplifier. The API documentation loosely groups channels into six main categories based on the type of inputs/outputs (IO) they provide. The main channel categories are listed in Table 3.

Table 3: DAQ Module Categories

Type	Input or output	Abbreviation
Analog	In	ai
	Out	ao
Digital	In	di
	Out	do
Counter	In	ci
	Out	co

3.2.2.5 *Naming Convention*

When interfacing with the NI-provided code libraries, the API will automatically assign a name to each of the components of the DAQ system based on when the components are detected by the computer. The API then concatenates the individual component names to build up the names of sub-component. For instance, the first chassis detected by the system will get the designator “cDAQ1,” the second chassis will get the designator “cDAQ2,” and so on.

³ For purposes of this report, the API can be thought of as the code library provided by NI to allow other programs the ability to interact with and control the DAQ devices.

The individual modules connected to the chassis have a similar naming convention. If a chassis has only one slot for a module, that module will be assigned the name “Mod1,” but if the chassis has multiple slots, then the module will be assigned a name based on which slot it is in. So, in a four-slot chassis with modules in the first and last position, the individual modules will have names “Mod1” and “Mod4” respectively.

Unlike chassis and module names which are one-indexed, channel names are zero-indexed. In addition, the channel name also indicates what type of channel it is, using the convention from Table 3. The result is a name such as “do0” or “ai15” for digital output 0 or analog input 15, respectively. The name that finally gets assigned to a given channel is a combination of the auto-generated names for the chassis, module, and channel. A possible result could be “cDAQ3Mod4/ai0,” where cDAQ3 indicates the third chassis connected to the system, Mod4 indicates the module connected to the 4th slot in the chassis, and “ai0” indicates analog input, channel 0.

This naming convention is relevant because the names for the chassis are completely dependent on the order in which they are detected by the system and can change depending on something as simple as the order in which the devices are plugged into the computer. This means that static references to a given channel name, such as might be in a configuration or test setup file, cannot be used. Any tool designed to interact automatically with specific physical channels has to implement a method of determining and validating channel names.

3.3 Test Fixture

Figure 16 shows the basic layout of the flicker testbed. An image of the actual test setup is given in Figure 17. There are five main stages to the fixture: signal creation and buffering, input signal digital to analog conversion, amplification, powering the light bulb, and capturing the light output. Each stage is described in Section 3.3.1. A listing of the test fixture hardware is given in Table 4.

Figure 16: Test Fixture Diagram

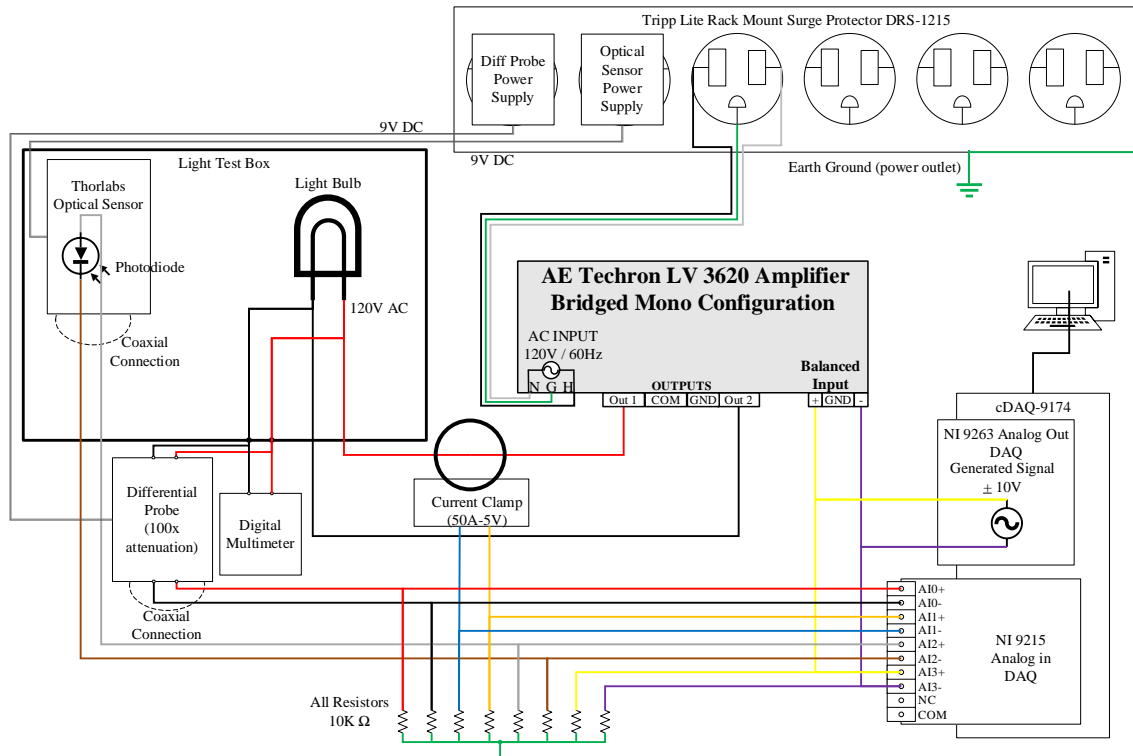


Figure 17: Flicker Test Fixture



3.3.1 Hardware Stages

3.3.1.1 Signal Creation and Buffering

The H5 toolchain pulls the signal data in from a pre-generated signal file (see Section 4.3.3) and pushes it to the DAQ analog output card. Due to the high sample rate and large file sizes associated with this test setup, the toolchain actively manages buffering data into and out of the DAQ.

3.3.1.2 Input Signal Digital to Analog Conversion

The NI 9263 Analog Output Card converts the digital data into an analog signal. This generated signal is directly monitored by the NI 9215 Analog Input DAQ and is listed as "Vin" on the recording data.

DAQ voltage limits: ± 10 V

DAQ sample rate: 100,000 samples/sec

Typical signal range for these tests: 1.2 V RMS (1 V peak * 1.705 scale factor)

3.3.1.3 Input Signal Amplification

The signal from the DAQ is sent into the balanced inputs on the Techron Amplifier, which then scales the input signal up to the range of 120 V RMS. To reach the required output voltage level, it was necessary to configure the Techron for "bridged mono output." In the bridged mono configuration, Output 1 comes from the Ch1+ terminal, Ch1- and Ch2+ are connected internally, and Output 2 comes from the Ch2- terminal [29]. This configuration places the outputs of both channels in series with each other and allows for much higher output voltage from the amplifier. Figure 18 shows the connections on the Techron outputs.

Figure 18: Techron Bridged-Mono Configuration



3.3.1.4 Powering the Light Bulb

The output signal from the Techron is fed into the bulb test box, where it is used to power the light bulb under test. The bulb test box consists of an opaque fiberglass enclosure containing a junction

box/socket for the bulb, the bulb itself, and the Thor Labs light sensor. The current and voltage being applied to the bulb are monitored using a current clamp and differential probe, the measurements of which are both fed into the analog input DAQ. The measured bulb voltage and current are listed as "Vbulb" and "Cbulb," respectively, on the recording data. In addition, a handheld digital multimeter is connected in parallel to the differential probe. The multimeter is included to provide live feedback on the voltage level applied to the bulb and to sanity-check measured values.

3.3.1.5 Capturing the Light Output

The light output from the bulb is captured using the Thor Labs light sensor. This sensor is, in essence, a specialized photodiode and amplifier that takes the irradiance incident on its lens and produces an output current proportional to the received energy. If the light sensor output is connected to a high impedance load—which is the case in this setup—the output current becomes minimal and the generated output voltage from the sensor becomes proportional to the energy received by the sensor input.

The analog values from the light sensor are captured and recorded by the analog input DAQ; this channel is listed as "Light" in the recorded data. For a more detailed assessment of the actual values being measured by the light sensor, see Section 5.2.

Note regarding captured signals

None of the recorded signals in the shown test setup have a ground reference, so they are effectively floating with respect to the analog input DAQ. Both the input and output DAQ cards are grounded via their USB connection to the computer but overall, the system did not have a reliable ground reference point. During initial testing, the lack of a ground reference resulted in significant issues where the recorded values would interact with each other or skew the relative ground level. These interactions gave the appearance that all the signal values were varying wildly over the course of several seconds. In order to establish a fixed ground reference, a 10 k Ω pull-down resistor was connected to the negative lead on each of the recording channels. These pull-down resistors were then connected at a single point, which was directly connected to the grounding screw on the test fixture power supply.

3.4 Equipment List

Table 4 provides the list of the exact equipment names and models used in the test fixture.

Table 4: Equipment List

Item	Manufacturer	Model	Description	Note	Source
Differential Probe	Pico Technology	TA041	25 MHz 700 V differential oscilloscope probe 10:1/100:1	100 V:1 V	[33]
Differential Probe	Teledyne LeCroy	AP031	OSCOPE PROBE X10/X100 25 MHZ 4M	100 V:1 V	[34]
DAQ (Output)	National Instruments	NI-9263	C Series Voltage Output Module	100 kS/s/ch Simultaneous, ± 10 V 4-Channel C Series Voltage Output Module	[29]
DAQ (Input)	National Instruments	NI-9215	C Series Voltage Input Module	± 10 V, 100 kS/s/ch, 16-Bit, Simultaneous Input, 4-Channel C Series Voltage Input Module	[30]
DAQ Chassis	National Instruments	cDAQ-9174	NI CompactDAQ Chassis	4-Slot, USB CompactDAQ Chassis	[31]
Current Clamp	Flex-Core	M1V-50-5	AC CURRENT MICRO CLAMP	50 A:5 V	[35]
Digital Clamp Meter	Fluke	324	True-RMS Clamp Meter with Temperature & Capacitance	Measures AC current up to 400 A Measures AC/DC voltage to 600 V	[36]
Light Sensor	THORLABS	PDA100 A2	Si Switchable Gain Detector	320 - 1100 nm, 11 MHz BW, 75.4 mm ²	[37]
Amplifier	Techron	LV 3620 ⁴	Linear Amplifier	1 V:100 V (bridged mono cfg.)	[32]
Incandescent	Feit Electric	100A/RS /TF-130	100-Watt Incandescent A19	Color Temp: 2700 K 92 W, 800 lm at 120 V	[1]
CFL	GE Lighting	FLE11/2 /A17XL/ SW Model: 47486	Energy Smart CFL 11 W (40-watt Replacement) A17 Light Bulb with Medium Base	Color Temp: 2700 K 11 W, 550 lm at 120 V	[38]
LED	Great Value	GVVLA 6027ND 4	Great Value LED Light Bulb, 9 W (60 W Equivalent) A19 Lamp E26 Medium Base, Non-dimmable, Soft White	Color Temp: 2700 K 9 W, 750 lm at 120 V	[3]
Halogen	GE Lighting	66279	PAR38 Halogen, Flood Light Bulbs, Warm White Spotlight, Indoor and Outdoor	Color Temp: 2900 K 60 W, 1070 lm at 120 V	[2]
Bulb Enclosure	Allied Moulded	AM120 6RT	AM-R Series fiberglass wall mount enclosure assembly	12"x10"x6" with raised hinged cover and stainless-steel twist latch	[39]

⁴ Technically the amplifier is an SEL 4800 model Techron, which is a special-built model using features of both the LV3620 and the LV3622. However, since that is not a commercially available product, it was necessary to use the specifications and documentation for the LV 3620.

3.5 Procedure for Conducting the Flicker Tests

3.5.1 Necessity of Bulb Warmup

Personal experience has shown that the output characteristics of a bulb are highly dependent on temperature. For example, when CFLs were first introduced to the market, it was common for the bulb to be extremely dim when first powered on, with the CFL only reaching full brightness after a few minutes of being on. In addition, early testing showed variations in light bulb responses over the course of longer tests, even if the difference was not visually obvious. In order to reduce any potential issues associated with changing behavior due to bulb temperature, it was decided that a ten-minute warmup sequence should be used before running any of the tests. This warmup sequence, in turn, added a new challenge of having to make sure the follow up tests were conducted immediately following the warmup. It was not practical or reliable to manually launch the tests, so it quickly became apparent that a scriptable method of launching tests was needed.

3.5.2 Preprocessing: Signal Generation

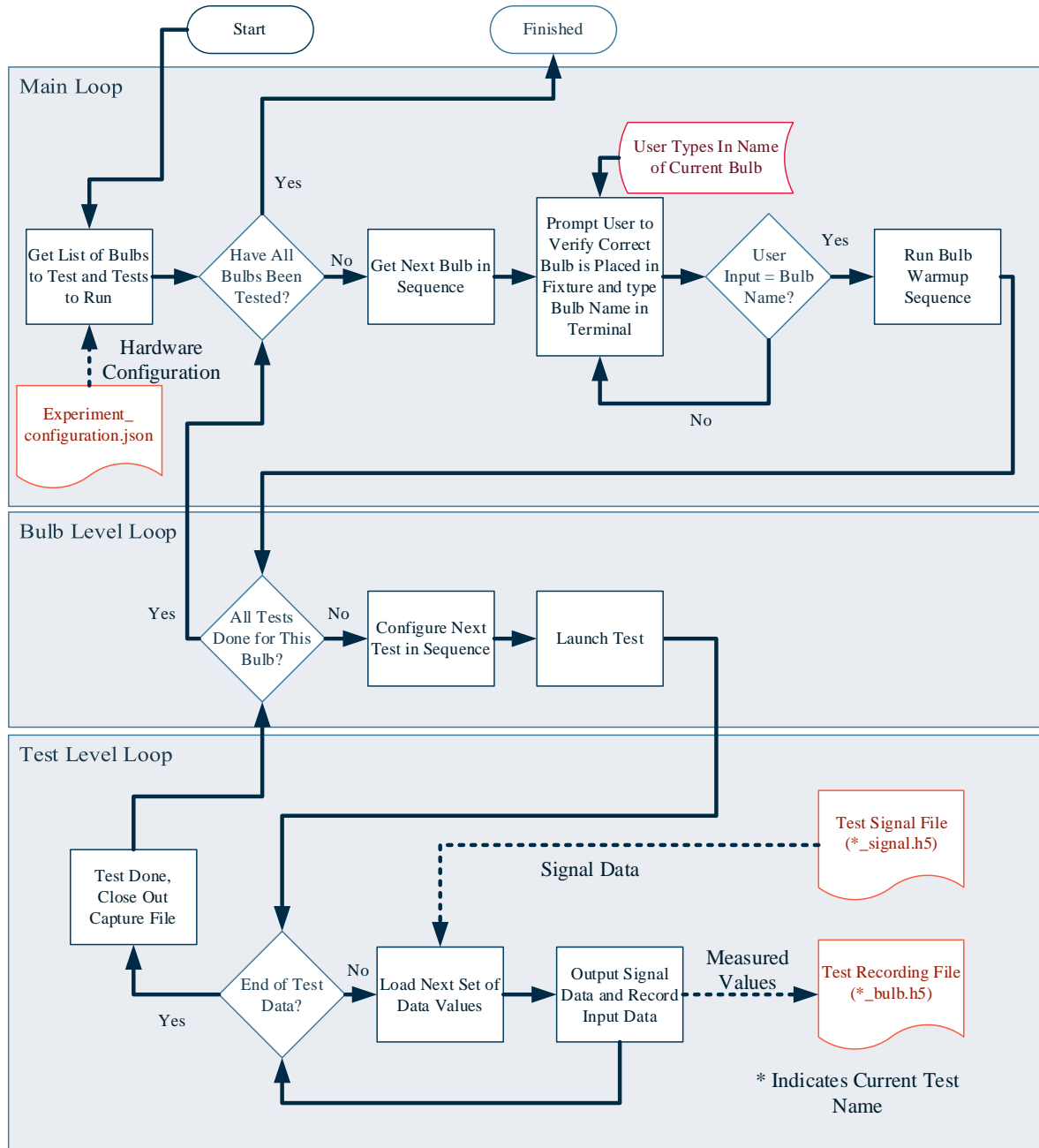
Before any tests can be run, signal sets need to be created that can be used as the inputs to the test sequence. The creation of these signal sets is handled by the H5 Signal Generator tool (see Appendix Section A.2). Pre-generating the input signal files provides the following benefits:

- It eases the processing burden on the computer that is driving the tests, especially since H5 files allow piece-wise file access, so the entire file does not need to be loaded into memory at one time (see Section 4.1.3 for more detail).
- Having the data pre-defined makes it possible to maximize consistency between different runs of a test or between tests of different bulbs.
- Multiple tests can easily be run sequentially by looping through a list of signal data files.
- When a given test is run, the input data is also included in the recording file. By including the generated data with the recorded data, a direct comparison can be made between the inputs and outputs of the test system.

3.5.3 Test Sequence

Figure 19 demonstrates the general sequence that was developed for conducting light flicker tests.

Figure 19: Test Sequence



As can be seen in Figure 19, the main testing process consists of several nested loops. The outermost loop goes through all the bulbs under test and ensures the warmup sequence is run on each bulb before the program enters the second, inner loop. The inner loop goes through every test in the desired sequence, ensures the necessary configuration and file setup processes occur for that test, and then enters the inner-most loop by launching the given test process. The inner-most loop runs the actual test in question, which consists of queuing up output data samples from that test's signal file and saving recorded input samples until the given test is complete.

The scripted sequence was set up such that the output files would be automatically named to indicate both the bulb and test, then placed into a results directory that had them sorted by test type. This allowed better organization of test results.

3.6 Summary

Though most flicker test setups share a similar basic structure, special care was still required to determine the specifics of which equipment to use, how to configure the setup, and what metrics should be the most relevant. The use of the NI DAQ series of devices allows for high-speed, high-resolution generation and capture of multiple data channels simultaneously. The tradeoff associated with using the NI DAQ system is that, while the devices are perfectly capable of generating and capturing data at the stated rate and resolution, it is on the user to figure out a method of handling and processing the large number of data samples. Developing those methods and tools essentially turned into an entire project in and of itself, as described in Chapter 4.

Chapter 4: Development of the H5 Toolchain

4.1 Project Background

4.1.1 Initial Data Capture Tools “SELDAQ” And “NIPlay”

When this research began, there were already some initial data output and capture tools in place for interacting with the NI DAQ equipment. Though they were never published or fully released, the data capture and data generation tools were known internally within SEL as “SELDAQ” and “NIPlay”, respectively. These tools, which had been developed internally by an engineer at SEL for internal use, served as a starting point for conducting the research. The examples of the graphical user interface (GUI) for SELDAQ and NIPlay are given in Figure 20 and Figure 21, along with a brief description of each.

4.1.1.1 SELDAQ

Figure 20: SELDAQ Tool [40]

Channel Configuration

#	Channel	Name	Scale	RMS
0	cDAQ3Mod4/ai0	Vbulb	100	0
1	cDAQ3Mod4/ai1	Cbulb	10	0
2	cDAQ3Mod4/ai2	Light	1	0
3	cDAQ3Mod4/ai3	Vin	1	0

Device Configuration

Duration: 600 sec Sample Rate: 100,000 sps

Output: C:\Users\ericjohn\Desktop\Example_Sf Browse...

Comment: |

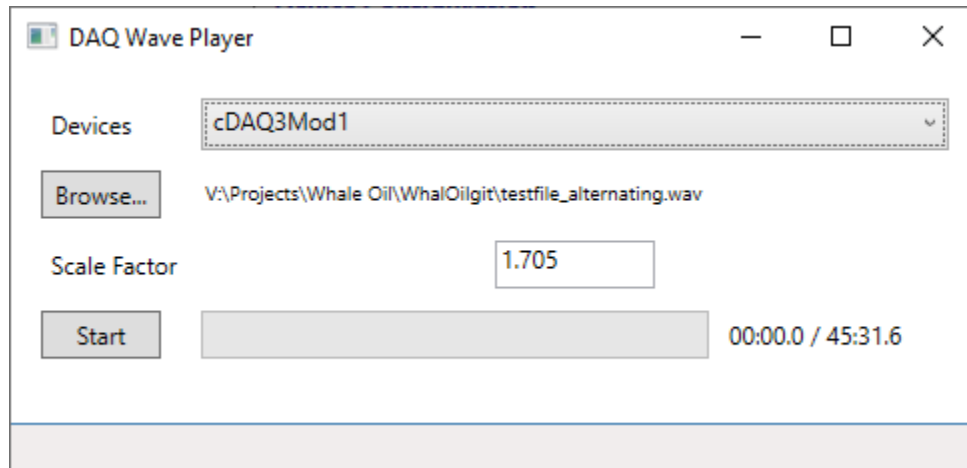
0:00:00.00 Go

All Good... v0.6

SELDAQ is a data capture tool designed to interface with NI DAQ equipment. Upon starting, the program will check to see if a compatible set of equipment is connected to the computer and will allow users to select available data channels from the dropdown menu near the top (grayed out in Figure 20). Selected channel names and scaling values can be configured using the table in the middle of the figure. The section near the bottom allows the user to control the recording configuration (including the sample rate for the data) the duration of the recording, the desired location of the output file, and any comments that the user wishes to include with the recording.

4.1.1.2 NIPlay

Figure 21: NIPlay Tool [40]



Though the GUI window displays “DAQ Wave Player,” Figure 21 shows the interface for the NIPlay tool. This tool was designed to be a simple method for producing a signal output with a DAQ, using a pre-generated signal file in .WAV format. The user can select a specific chassis/module combination from an automatically populated list of available output devices, select a .WAV file, and provide an output scaling factor. The tool will then output the signal data on the first channel of the selected module.

4.1.1.3 Limitations of the Initial Tools

SELDAQ and NIPlay were highly useful tools, and they provided sufficient functionality to get the testbed functional as well as some initial flicker investigation. Ultimately, though, some limitations with the tools became apparent and began to hinder and block further research progress. These limitations include:

Inability to script interactions or test sets: In order to run any given test, the output file had to be selected using the “Browse...” button and the file selection dialog box on the NIPlay GUI. This made it impossible to run a series of back-to-back tests. In addition, all the test signal files had to be manually generated ahead of time. The signal generation was typically done in python by generating a data array of the desired signal, then exporting it to a .WAV file.

Recording file paths had to be manually updated: The SELDAQ tool did not allow for automatic creation of output file paths. So, if multiple sequential tests were to be run, the user would have to remember to update the output path between tests or risk overwriting the results of the previous test.

Generation and capture were completely decoupled: While the ability to play and record independently of each other does have useful applications—often a user only needs to do one or the other, not both—it poses a substantial challenge when a test calls for generating an output and immediately recording a system’s response to that output. For initial testing, it was necessary to have both GUI windows open, configured, and positioned right next to each other on the computer monitor. The user would then launch the record process, then rapidly switch over to the play tool, and click “run” on the play process. The time necessary to move the cursor from the “record” button on the SELDAQ tool to the “run” button on the NIPlay tool would inevitably result in a second or two of dead time on the input file, followed by a startup transient as the output DAQ began to play. The user would then have to go in and manually trim off the dead time, and possibly the transient before any meaningful analysis could be performed.

NIPlay tool did not have channel options: Though it was not relevant to this specific research project, the inability of the NIPlay tool to interact with more than one channel when generating a signal was a severe limitation for any user who wished to generate multi-channel data such as stereo signals or a simulated three-phase power waveform.

4.1.1.4 Shifting Research Focus

Overall, if the user was just trying to accomplish simple, one-off tests, then the existing tools were quite useful and sufficient. However, once the testbed was functional and the research started requiring multiple sequential tests, then the existing process and tools became inefficient, tedious, and error prone. The ability to script test sequences became increasingly appealing, and the nature of the research started shifting. At first the focus was on capturing and analyzing light bulb flicker. Before that could happen, however, there needed to be tools that could do the generation, capture, and analysis.

4.1.2 Why Use Python?

The original versions of the DAQ tools, as described in Section 4.1.1, were written in C#, but the decision to implement the versions in python came down to several factors:

- C# tends to be heavily coupled with Microsoft, whereas python code can be used on a wide variety of operating systems and devices.
- The NI DAQ API was supported in both C# and python, so neither language appeared to have a distinct advantage over the other in regard to interacting with the NI libraries.
- This was an excellent opportunity to gain experience in using python.
- The work team was starting to make the shift towards doing new projects in python, and most of them had already been working with it extensively, so developing the updated tools using python would help keep our project base consistent.

4.1.3 Why Use HDF5?

Table 5: Advantages and Disadvantages of Different Data Storage File Types

File Type	Ext	Advantages	Disadvantages
Comma separated values	.csv	<ul style="list-style-type: none"> • Human readable • Supported by numerous tools (text editors, Microsoft Excel, python, etc.) 	<ul style="list-style-type: none"> • ASCII encoding scales poorly with large data sets • Reading and writing are slow • Limited ability to store metadata or distinguish data sets.
Excel	.xls .xlsx	<ul style="list-style-type: none"> • Commonly used in a wide variety of industries 	<ul style="list-style-type: none"> • Slow file read/write operations • Worksheets have an absolute maximum number of rows and columns [41] • Automatic formatting can change source data [42]
Feather		<ul style="list-style-type: none"> • Very fast file read and write access 	<ul style="list-style-type: none"> • Not quite as widely supported
Other serialized data formats (JSON/YAML/XML)		<ul style="list-style-type: none"> • Human readable • Widely supported 	<ul style="list-style-type: none"> • Slow read and write operations • Limited data compression capability
Hierarchical Data Format (HDF)	.h5 .hdf5	<ul style="list-style-type: none"> • Allows for storage of arbitrary data, including distinct data sets and metadata • Values are stored as binary, allowing for much quicker read/write operations • Data compression allows files to be much smaller • Elements can be accessed without loading entire file into memory 	<ul style="list-style-type: none"> • Not human readable • If files are not closed correctly, they can be corrupted

According to the HDFGroup website [43]:

"HDF5 is a data model, library, and file format for storing and managing data. It supports an unlimited variety of datatypes and is designed for flexible and efficient I/O and for high volume and complex data. HDF5 is portable and is extensible, allowing applications to evolve in their use of HDF5."

Ultimately, the decision to use HDF5 files for data storage came down to several factors

- Ability to make nested data structures (akin to a file system or dictionary in python)
- Ability to read/write chunks of data without having to load the entire file into memory
- Compatibility with other tools that had already been developed by our team

The specifics of how the HDF5 Tools function is outside of the scope of this report, but a brief description of a number of these tools is provided in Section 4.3.

4.2 The Need for a New or Expanded Framework

As initial attempts to modify the tools to make them more scriptable proved unsuccessful, it became clear that the existing tools were not going to be sufficient. The tools were so closely integrated with their respective GUIs that attempting to decouple the tool from the GUI would likely take as much time and effort as writing a new tool from scratch. Also, the tool was not architected to support a growing list of desired features, such as those listed in Section 4.2.1.

4.2.1 Requirements for the Improved Framework

Attempting to debug the test setup, perform initial captures, and ultimately develop an expanded tool for interacting with the DAQ system showed that this new tool had to have the following requirements:

Consistent and clear signal/test file generation: Manually generating the data arrays had proven to be a tedious and error-prone process, and there was no clear or consistent way to document exactly what values had been injected into a given test set, aside from embedding a description in the test file name. There needed to be a way to generate test data sets quickly and consistently. Ideally, the user would be able to describe the desired test attributes—duration, frequency, amplitude, phase shift, additional noise, etc.—and the tools would build up a signal file from those attributes.

Scriptable interactions: It had to be possible to script the test interactions so that one test could be launched immediately following the previous test. Initial attempts to manually launch tests after a ten-minute warmup sequence had been extremely unreliable, and the general goal was to be able to generate an arbitrary number of different test cases, run them all in sequence, and then repeat for each bulb under test.

Ability to propagate metadata: When analyzing the output of a test system, it is extremely useful to have a clear reference as to what inputs generated the given outputs, as well as some indication of what the test was trying to see or accomplish. This feature ties in with the signal file generation capability listed above. The goal is for a user to be able to define a set of test data—ideally including a brief description of the test itself—using some human-readable format, generate a signal set from that definition, run a test, and then have all of that information about the initial test propagate into the results file.

Data analysis and plotting tools: Previous projects had shown just how tedious and time consuming it can be to create and manipulate plots for displaying data sets. Having a set of tools to automatically generate common plot types—such as time domain plots, filter outputs, spectrograms, etc.—from the recorded data sets would significantly improve efficiency when trying to analyze test results.

Ability to adjust result file attributes after the fact: Even with increased scriptability and automation when conducting tests, there is often a need for tools to manipulate or adjust the results file after the test is done. The needed action could be as simple as updating the name on a metadata field, or it could be a more complicated action such as trimming startup transients out of the actual data set.

4.3 Combining Parts to Build a Versatile Test Toolchain

Upon conferring with the rest of the work team about the requirements for the new testing framework, it was discovered that many of them had been independently working on python-based tools to address similar issues. The project briefly became a large collaborative effort as the entire group worked to integrate their individual tool components. Like the folk tale “Stone Soup,” where hungry travelers were able to create a feast for a community by getting small contributions from individuals [44], the toolchain for generating, capturing, displaying, and analyzing data came together from a number of small tools written by individuals.

The sections below provide a brief description of each of the relevant tools, as well as an explanation of what each tool does to address the requirements from Section 4.2.1.

4.3.1 H5Model⁵

The core of the entire toolchain is the H5 model. It provides a consistent framework and interface for interacting with HDF5 files. Everything else in the toolchain operates using the H5 model for storing, processing, and writing data. The model is largely behind the scenes for most interactions, and the user will typically only interact with the model format when they want to inspect the contents of a given file or dataset. The main way the H5 Model supports the listed requirements from above is by providing a framework and storage methodology for all the information associated with a given signal or recording. Examples of the layout and components associated with the H5Model format are given in Section A.1.

4.3.2 H5Convert⁶

The H5Convert tool is only loosely associated with the light flicker research. The purpose of this tool is to support conversion of different file types to and from the H5Model format. By converting a file or dataset to the H5Model format, the user can then apply the other tools in the H5 library, such as plotting and signal generation. This tool can already support a wide variety of file types, including audio (.WAV), Comtrade (.CFG, .CFF), comma separated values (.CSV), and Electromagnetic Transients Program – Alternative Transients Program (EMTP-ATP) files (.PL4). Other supported file types are being added on an as-needed basis. Because all the flicker research is already based on the H5Model format, the H5Convert tool is of limited use in this project's particular research.

4.3.3 H5Signalgen⁷

The H5Signalgen tool is designed to be able to take a text-based description of the characteristics of a signal set and use that to generate a file containing that signal set, as well as other associated data, such as a description of the signal set, the signal sample rate, and the units, size, and name of each data set. One of the key desired features for this research was the ability to generate test waveforms rapidly and consistently. By describing the characteristics of the desired waveforms in a .JSON file, it is possible to quickly build up test signals that can then be generated and played out via the NI DAQ analog output card. For purposes of convention, all the signal files used in this experiment were given the "_signal" suffix in their file name.

⁵ Contributor(s): Thomas Halstead

⁶ Contributor(s): Ammon Kunsler and Joe Ferguson

⁷ Contributors(s): Eric Johnston, Tracy Young, Joe Ferguson

4.3.4 H5NIDAQ⁸

The H5NIDAQ tool was by far the most involved tool in the H5 toolchain, in terms of time and effort. This tool handles all the direct interaction with the NI DAQ platform when doing data generation, capture, or both, as well as managing/validating device configuration, controlling file input and output, and propagating configuration values and metadata to any recording files. The H5NIDAQ tool operates using its own kind of .JSON file, which describes the physical hardware setup for a given experiment, as well as what signal files, if any, to use. By either modifying the .JSON values or launching the tool using different command line arguments, it is possible to script a series of experiments to run sequentially. When creating output signals, the tool operates directly using the generated signal files from the H5Signalgen tool.

4.3.5 H5Plot⁹

This tool provides utilities for plotting datasets using the H5Model framework. The plotting tool provides the ability to generate time domain plots, frequency domain plots, spectrograms, and a variety of filter plots with a single function call for each. In addition, the user can plot every dataset and channel present in a given H5Model, or they can specify a subset of values to plot. It is also possible to create custom filters and plot types for this tool, so the plotting options can be tailored to the specific project requirements.

4.3.6 H5Tools¹⁰

H5Tools is a collection of various tools and utilities for modifying parts of the H5 files. Using the utilities associated with H5Tools, a user can merge different data files, split a multi-channel file into multiple files with single channels, trim off sections of data captures, etc. This tool directly addresses some of the more advanced file manipulation requirements listed in Section 4.2.1.

⁸ Contributors(s): Eric Johnston, Tracy Young, Joe Ferguson

⁹ Contributors: Joe Ferguson, Eric Johnston

¹⁰ Contributors: Joe Ferguson, Eric Johnston

4.4 Conclusion

Though it started out as a single project to investigate light flicker, this research culminated in the creation of a library of tools that could be applicable for a wide range of research topics and data analysis. The flicker research and its associated requirements, acted as the catalyst to combine a number of different individual tools into one combined tool set. On the whole, the tool library was a collaborative effort featuring the work of our entire team. It was developed because we, as a group, were repeatedly encountering situations where we had to generate, capture, process, convert, or display data in various formats. Over time it became abundantly clear that having consistent tools for doing data science operations—regardless of the origin of said data—would be highly valuable.

Chapter 5: Results

5.1 Introduction

As previously stated, this research topic initially had been focused on trying to evaluate and understand flicker in various types of light bulbs. However, as the research progressed, it became clear that before any kind of meaningful analysis could occur, there had to be a reliable and consistent way to record and display the captured data. In the end, the main result of this research is the existence of a tool set that is capable of capturing, displaying, and analyzing data from the flicker testbed. The following sections demonstrate a method to effectively display and analyze flicker behavior in various kinds of light bulbs, though the actual analysis remains part of future research (see Section 6.3).

5.2 Explanation of Measurements for Thorlabs Light Sensor

“Before you go WHALING AWAY with a bunch of math, stop and think!”

– Professor Dennis Sullivan

As referenced in Section 2.3.7 and Section 3.3.1.5, it is not trivial to perform an exact quantization of values and units during the conversion chain from applying voltage to the light bulb to recording the values from the light sensor. To completely map the energy applied to the bulb to energy output from the sensor, it would, at minimum, be necessary to account for the following:

- The power-to-light conversion efficiency of each individual bulb
 - The bulbs list their power consumption, lumens, and color temperature, but that is not nearly specific enough for actual analysis
- The spectral distribution of each bulb would likely need to be individually measured, which is not currently possible with available equipment
- The internal geometry and reflective properties of the test fixture
 - Direct irradiance onto the sensor will impart different energy than reflected light.
 - Most of the bulbs are the same size, but the halogen bulb is substantially larger and shines more directly into the sensor
 - The material of the box influences the spectral distribution of energy
- The spectral sensitivity and optical properties of the sensor
 - Different frequencies of light will be more readily absorbed by the sensor
 - The optical properties of the sensor lens are also likely relevant

It is not possible to quantify several of the above factors with the currently available test setup. Some of the measurements, such as luminous output, require highly specialized—not to mention physically large and carefully calibrated—test fixtures in order to be accurately measured [9]. Fortunately, the interest of this research is purely on how the inputs to the system (voltage and current) relate to the outputs of the system (voltage). Specifically, the research focuses on what effect a given modification of the input (noise frequency/amplitude, etc.) has on the output.

The test fixture itself can be abstracted as follows:

- 1) Power (W) is applied to light bulb
- 2) Light bulb generates an output that, through its own spectral properties and the geometry associated with the given bulb and fixture, results in a given irradiance (W/m^2), on the input of the sensor.
- 3) The sensor, which has a fixed aperture area (m^2), responsivity (A/W), and output gain (V/A)¹¹ converts the received irradiance into a voltage value that can be recorded by the DAQ.

The setup can therefore be treated as a converter that, for a given bulb, will result in a “volts and current in \rightarrow volts out” relationship that can then be modeled to determine relative effects between input and output. This generalization does limit the absolute accuracy of the measured data, future research could work to improve the accuracy and create a more exact method of following the energy conversion process (watts to lumens to joules and back to watts) but a substantial redesign of the test fixture would be required. See section 6.3.2 for more information.

5.3 Data Capture and Plotting

The following sections demonstrate several different sets of tests that were performed using the H5 toolchain. Each test is briefly described, and several sample output plots are presented. The tests were created using the H5Signalgen tool, captured using the H5NIDAQ tool, and plotted using the H5Plot tool.

In addition, a combined dataset for each test type was created using the utilities provided in H5Tools. For the combined datasets, the respective V_{bulb} , C_{bulb} , Light, and V_{in} channels for each bulb type in a given test were combined into a single file and dataset. Most of the combined files consist of

¹¹ Most of the datasheet is worded in such a way as to indicate that watts received typically correlates to output current, since the sensor is, at its core, a specialized photodiode. However, the test setup has the output of the sensor fed into a high impedance load, specifically the input of the DAQ. The high impedance limits the current and instead causes the output to manifest as a measurable voltage.

sixteen channels of data—one test with four data channels per test for each of four bulbs. The combined file for the Single Tone Injection (STI) test, which has nearly three hundred channels, is a notable exception (see Section 5.3.4 for more details). The combined dataset files allow for a direct comparison of bulb behavior for a given test.

The following tests and examples highlight interesting behavior and demonstrate the ability of the H5 toolchain to generate useful plots with only a single function call. It should be made clear, however, that the plots themselves are only an example of the ability to process data and generate outputs. The plots do not represent a full analysis of any attribute or behavior; any observed trends would benefit from further validation, and all the visualizations are in their default, unadjusted state.

5.3.1 Common Test Attributes

All the tests had several attributes in common. Most of the common attributes were set so as to produce a 120 V_{RMS}, 60 Hz sinusoidal voltage across the inputs of the bulb under test. Other attributes, such as the amplitude of the injected noise, were held constant to provide consistency between initial tests, but were intended to be adjusted during later stages of testing. The following list shows the values that were held consistent between test types:

- Fundamental Frequency: 60 Hz
- DAQ fundamental signal magnitude: 1.20 V_{RMS}
- Injected noise amplitude: 5% of fundamental
- Amplifier gain 100x
- Voltage applied to bulb (not including injected noise) 120 V_{RMS}

It should also be noted that the first 0.25 s of data have been trimmed from all the plots showing combined data from multiple bulbs. The plots were trimmed to reduce the plotting effects of startup transients on data analysis, as well as to highlight the “trimming” capabilities of the H5 tools.

5.3.2 Frequency Sweep

The first test that was conducted was a frequency sweep of the each of the bulbs. The goal of this test was to generate an approximate frequency response of each bulb, so that the scope of future tests could be narrowed to frequency ranges of interest.

5.3.2.1 Test Description

The overall test duration was 30.0 s, consisting of four seconds of 60 Hz signal with no additional noise. After the four second start time, a series of noise signals were added into the main signal. The frequencies, start times, duration and amplitude of the injected noise signals are given in Table 6.

Table 6: Frequency Sweep Noise Signals

Frequency	Start Time	Duration (s)	Amplitude
70 Hz	4.0 s	2.0 s	5 %
100 Hz	6.0 s	2.0 s	5 %
500 Hz	8.0 s	2.0 s	5 %
1000 Hz	10.0 s	2.0 s	5 %
2000 Hz	12.0 s	2.0 s	5 %
4000 Hz	14.0 s	2.0 s	5 %
8000 Hz	16.0 s	2.0 s	5 %
16000 Hz	18.0 s	2.0 s	5 %
32000 Hz	20.0 s	2.0 s	5 %
48000 Hz	22.0 s	2.0 s	5 %

Some relevant output plots for this test sequence are shown in the sections to follow.

5.3.2.2 Time Domain Plots

The following plot shows the time domain values that were recorded during the frequency sweep test on the incandescent bulb.

Figure 22: Time Domain Capture for Incandescent Frequency Sweep

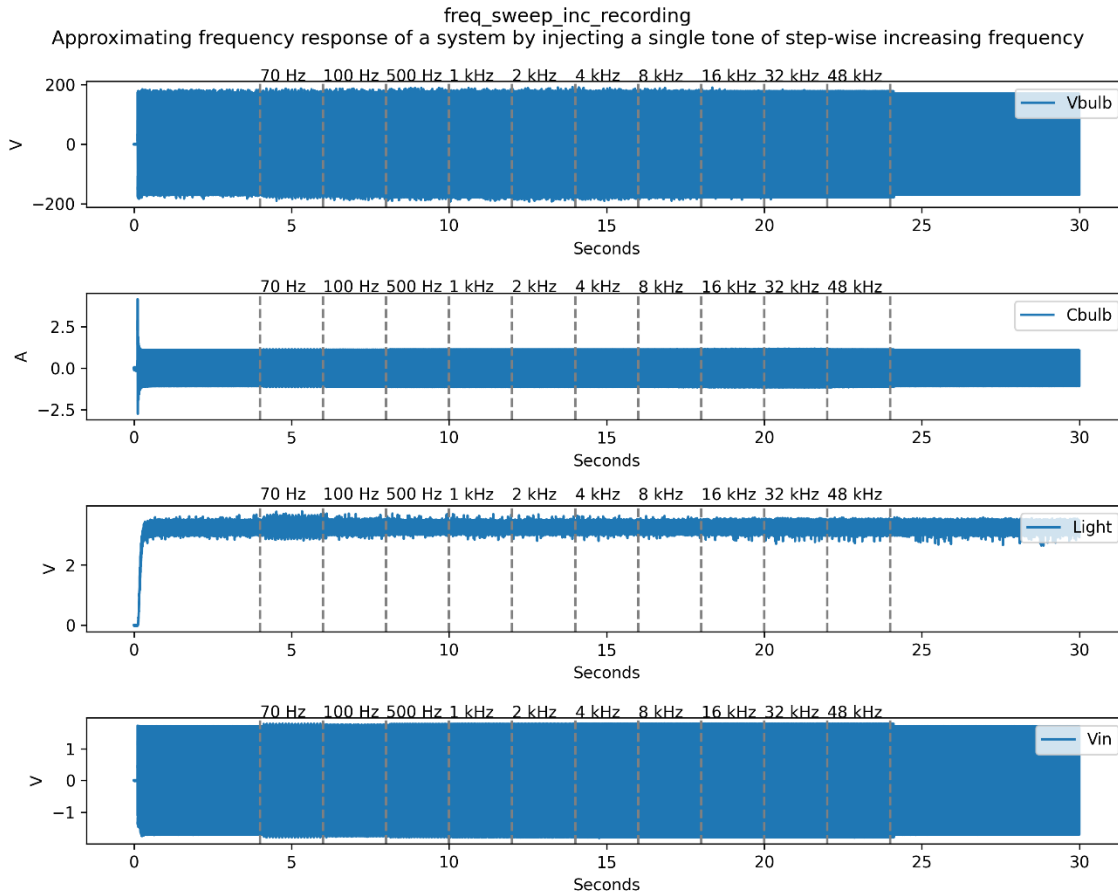


Figure 22 shows four subplots with the individual channel data for the voltage applied to the light bulb, the current going through the light bulb, the measured light output from the bulb, and the voltage applied to the input of the amplifier, listed as “Vbulb,” “Cbulb,” “Light,” and “Vin,” respectively.

Several interesting features can be observed in Figure 22. One of the most notable features is the visible change in light output from the bulb during the interval from four seconds to six seconds. Corresponds to the time frame where the 70 Hz noise signal is being applied. The notable distortion strongly indicates that further research is warranted with injected noise in the 70 Hz range.

Figure 23 shows the light outputs from each bulb during the frequency sweep test.

Figure 23: Time Domain Capture for All Light Channels During Frequency Sweep Test

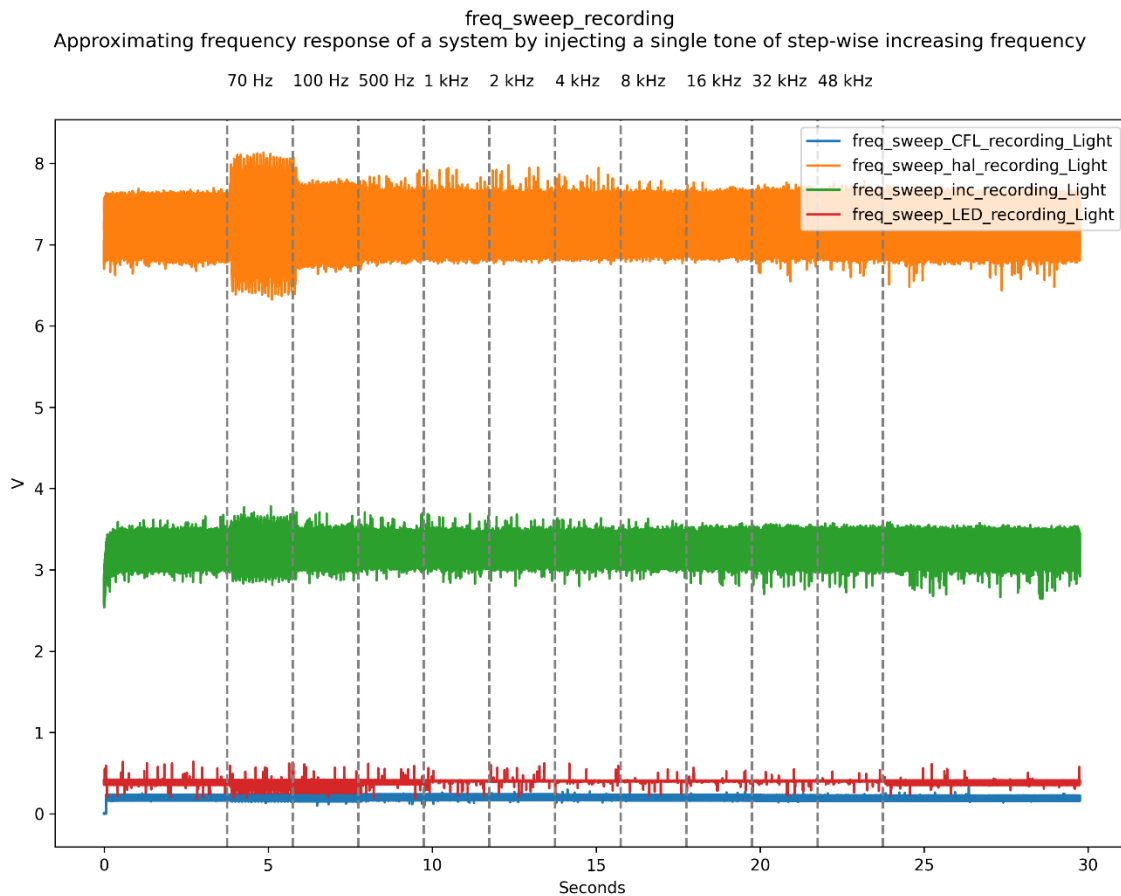
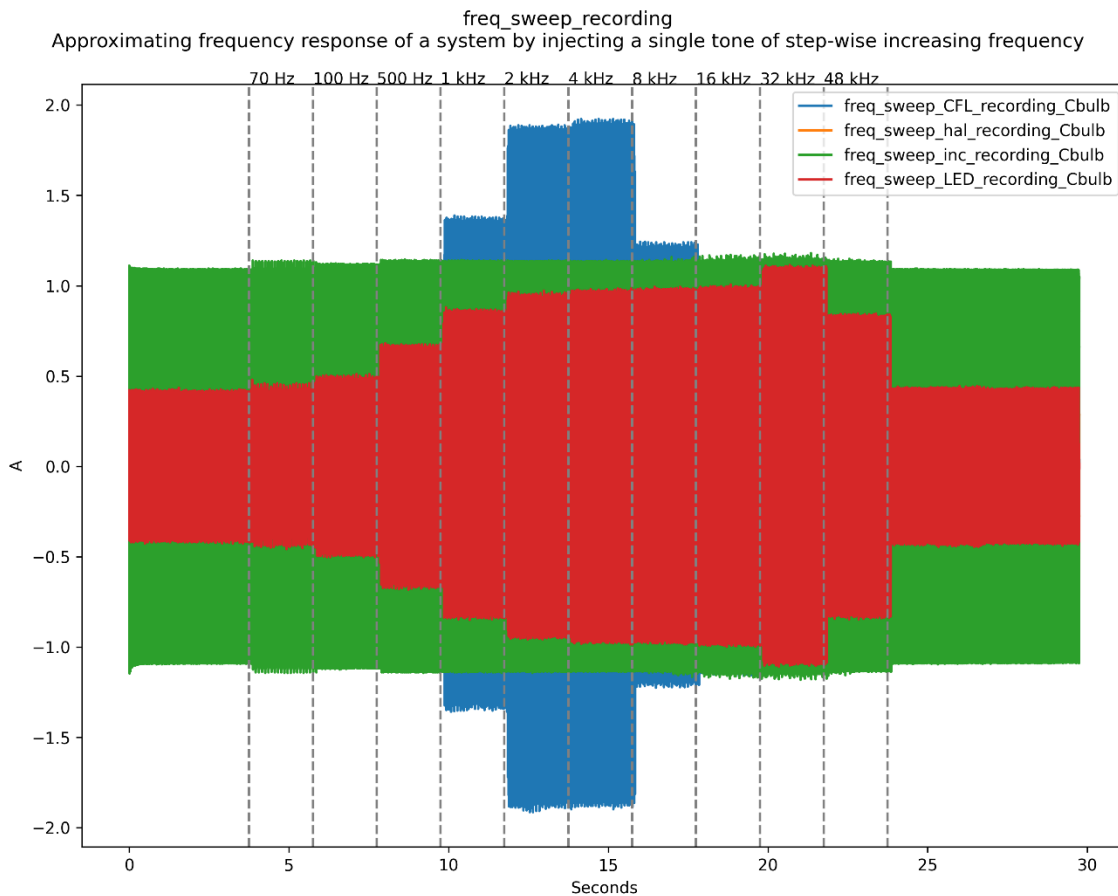


Figure 23 demonstrates several interesting features. The first notable feature is the amplitude differences between the measured light values for the different bulbs. As shown in Table 4, the halogen, incandescent, CFL, and LED bulbs have lumen ratings of 1070 lm, 800 lm, 550 lm, 750 lm, respectively, as well as differing geometry and spectral distributions, so the difference in output is expected, but still notable. The main takeaway from this feature is that in order to do a meaningful comparison between bulb output values, it will likely be necessary to normalize the channels.

The second interesting feature is the presence of a noticeable increase in output variation during the 70 Hz section of the test, as was also seen in Figure 22. The magnitude of the distortion is substantially more visible for the halogen and incandescent channels, but once again it is difficult to do a direct comparison. Some variation is visible during the 100 Hz segment as well, particularly for the LED channel. This feature reinforces the need for further testing in the range near 60 Hz.

Figure 24 shows the measured current through each bulb during the course of the same test.

Figure 24: Time Domain Capture for All Current Channels During Frequency Sweep Test



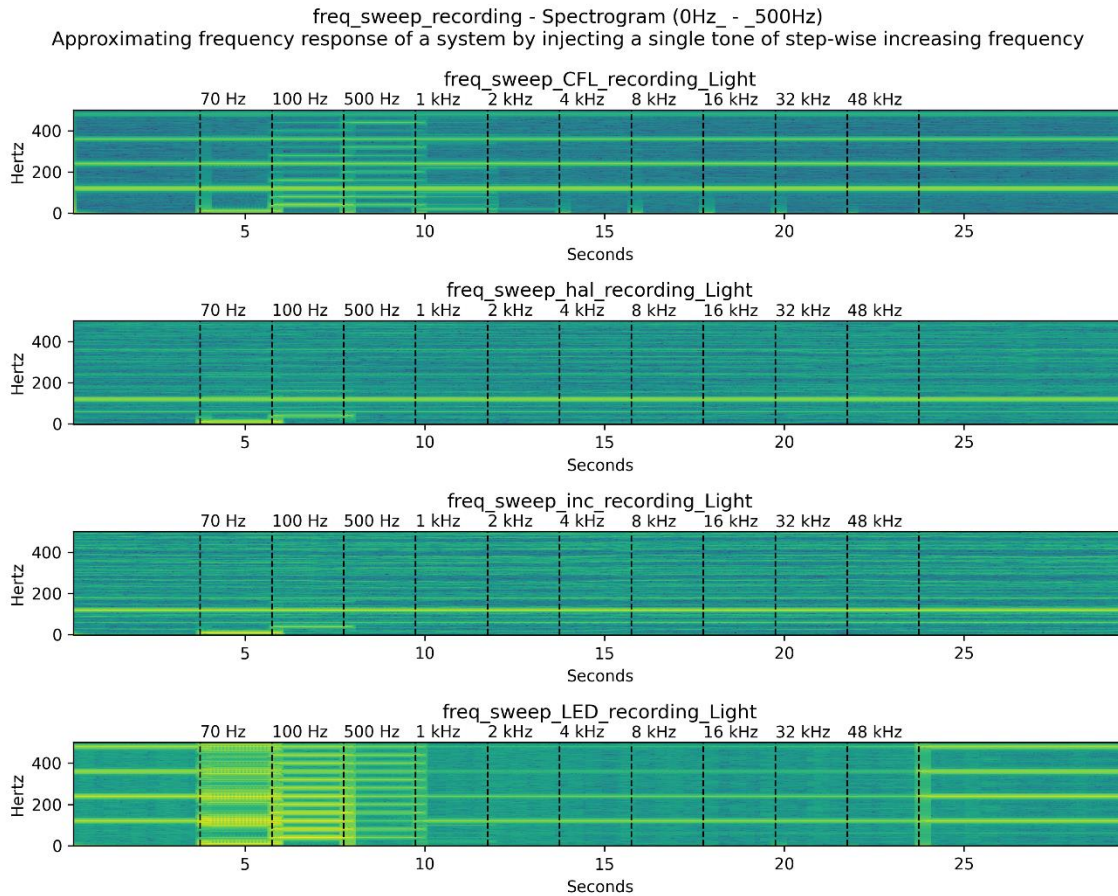
The main attribute of note in Figure 24 is the drastic increase in the current draw by both the CFL and LED bulbs as the frequency increases. Comparing with Figure 23 shows that the increased current does not correlate to an increase in light output. By contrast the incandescent current draw is relatively constant, as is the current through the halogen¹². One hypothesis is that the CFL and LED bulbs were experiencing a resonant effect in some frequency ranges, with the resonant effects decreasing as the frequency passed beyond the resonant range. Further research is necessary to determine the cause of the additional current and if the increased current causes additional problems such as excessive heating.

¹² Halogen current is not visible in this plot, but the relative consistency was verified by separately plotting the bulb current. The verification plot was omitted as it had very little overall contribution to the report.

5.3.2.3 Spectrogram

Figure 25 shows the spectral content of each bulb's respective light output over the course of the test. The frequency range for the spectrogram is specifically cut off at 500 Hz to allow the low-frequency behaviors to be more visible. The trade-off for better low-frequency visibility is that any of the signals injected after ten seconds into the test will be outside the range of the plot.

Figure 25: Spectral Response for All Light Channels During Frequency Sweep Test



The plots in Figure 25 exhibit several notable features. The first feature of note is the high harmonic content present in the LED and CFL captures. While the incandescent and halogen bulbs demonstrate clear bands at multiples of the fundamental frequency (180 Hz, 240 Hz, etc.), the banding feature is much more pronounced in the CFL and LED data sets. In addition, the injected noise signal also generated substantial harmonic content in the LED and CFL bulbs during the 70 Hz – 500 Hz segments of the test. It should be noted, however, that the above plot is another example where the lack of data normalization may be skewing the results.

5.3.3 Frequency Toggle

While the frequency sweep of Section 5.3.2 was useful for gaining insight into the frequency-dependent behavior of the different bulbs, it was often difficult to tell if an observed effect was related to the injected noise. The frequency toggle test was developed to try to establish a much stronger relationship between an injected frequency and an observed output by switching back and forth between two different noise frequencies.

5.3.3.1 Test Description

The overall test duration was 30.0 s, consisting of five seconds of 60 Hz signal with no additional noise. After the five second start time, a 70 Hz tone was injected for five seconds, then a 200 Hz tone for another five seconds. The 70 Hz, then 200 Hz, sequence was repeated one more time before the signal concluded with a final five seconds of just 60 Hz. The frequencies, start times, durations, and amplitudes of the injected noise signals are given in Table 7.

Table 7: Frequency Toggle Noise Signals

Frequency	Start Time	Duration (s)	Amplitude
70	5	5	5%
200	10	5	5%
70	15	5	5%
200	20	5	5%

Some relevant output plots for this test sequence are shown in the sections to follow. To better distinguish between periods of 70 Hz injection and the periods of 200 H injection, dashed lines and frequency labels have been added to each of the plots. These lines indicate the time periods where a given frequency is being injected, and the labels indicate which frequency is being injected.

5.3.3.2 Time Domain Plots

Figure 26 shows the time domain values that were recorded during the frequency toggle test on the incandescent bulb.

Figure 26: Time Domain Capture for Incandescent Frequency Toggle

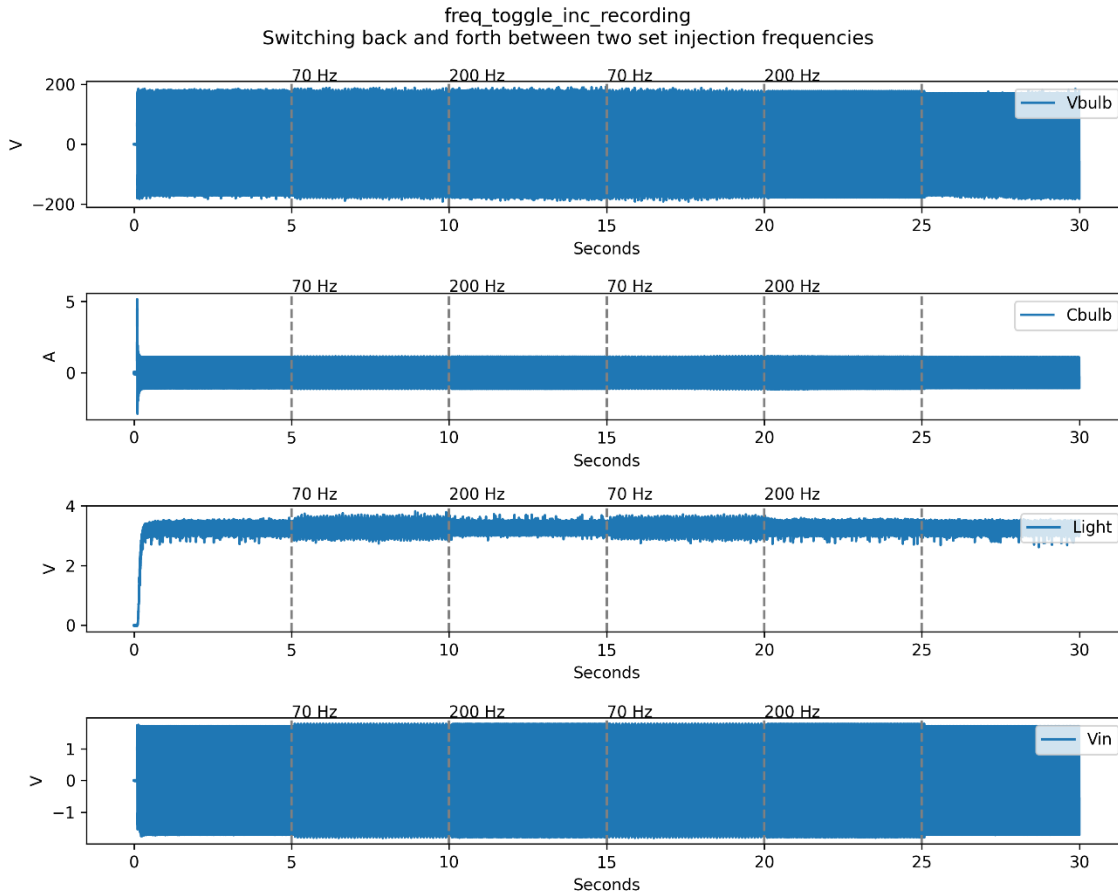


Figure 26 shows similar behaviors to the single bulb time domain plot from section 5.3.2.2. Once again, the increase in light amplitude variation is visible during the 70 Hz injection, and some variation is visible in the voltage and current channels during both the 70 Hz and 200 Hz segments. The voltage and current variation are most noticeable at the beginning and end of the noise injection sequences.

Figure 27 shows the light outputs from each bulb during the frequency toggle test.

Figure 27: Time Domain Capture for All Light Channels During Frequency Toggle Test

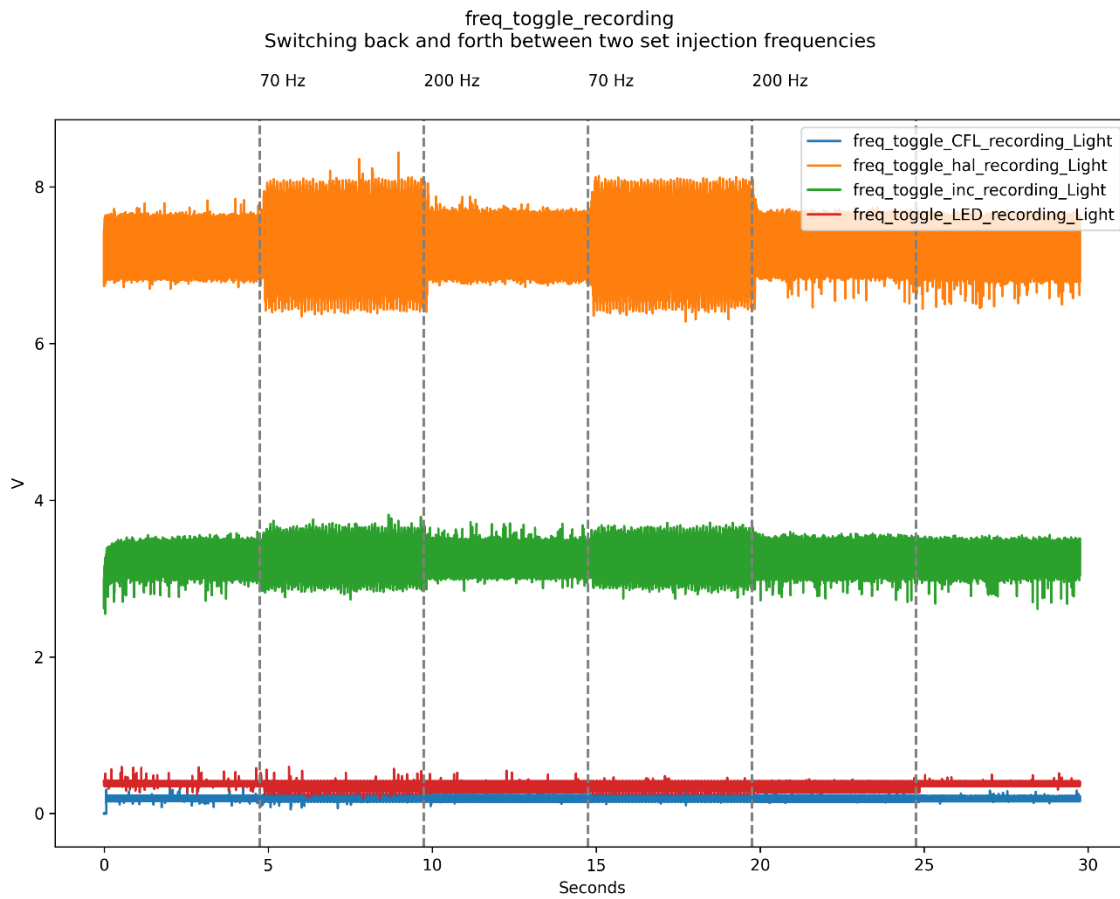


Figure 27 shows that, like in the frequency sweep test, all the bulbs demonstrate noticeable output variation when 70 Hz noise is applied. In addition, the LED and CFL bulbs show output variation when 200 Hz noise is applied as well; this effect may be present in the incandescent or halogen bulbs, but it is not as visible.

5.3.3.3 Spectrogram

Figure 28 shows the spectral content of each bulb's respective light output over the course of the test.

Figure 28: Spectral Response for All Light Channels During Frequency Toggle Test

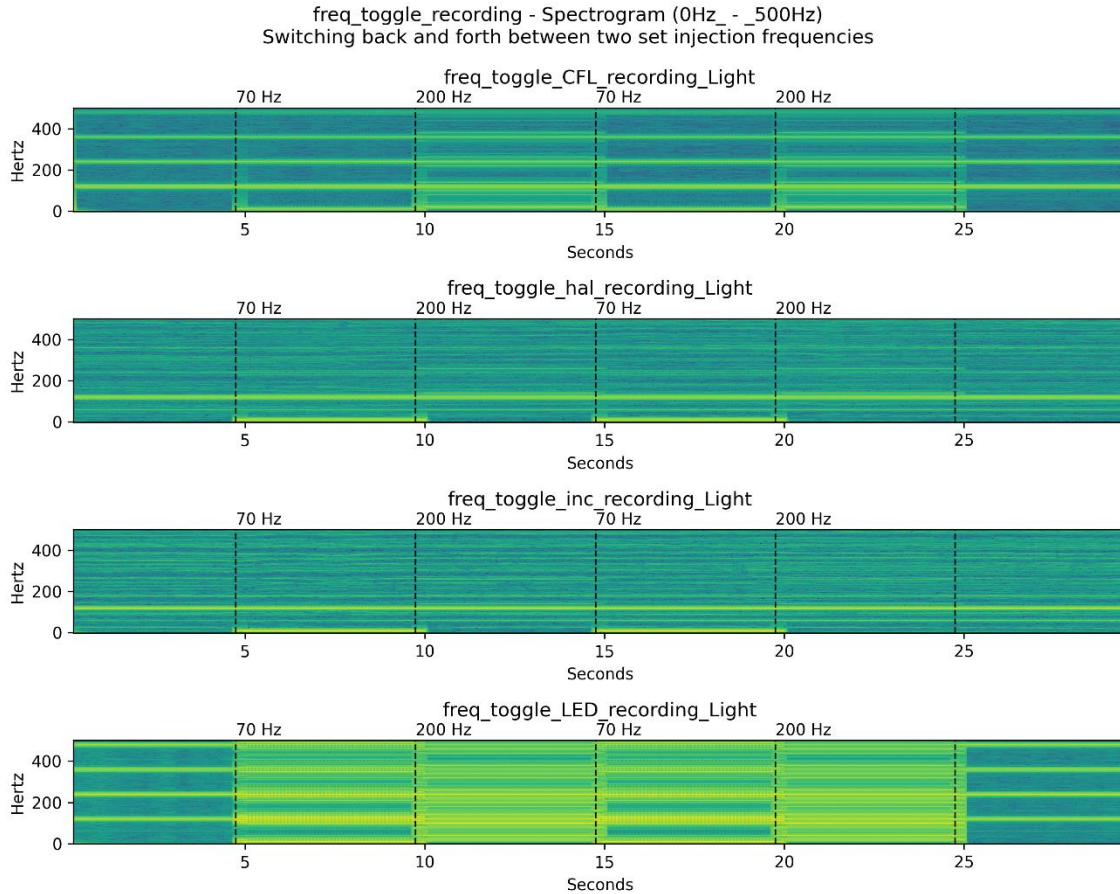
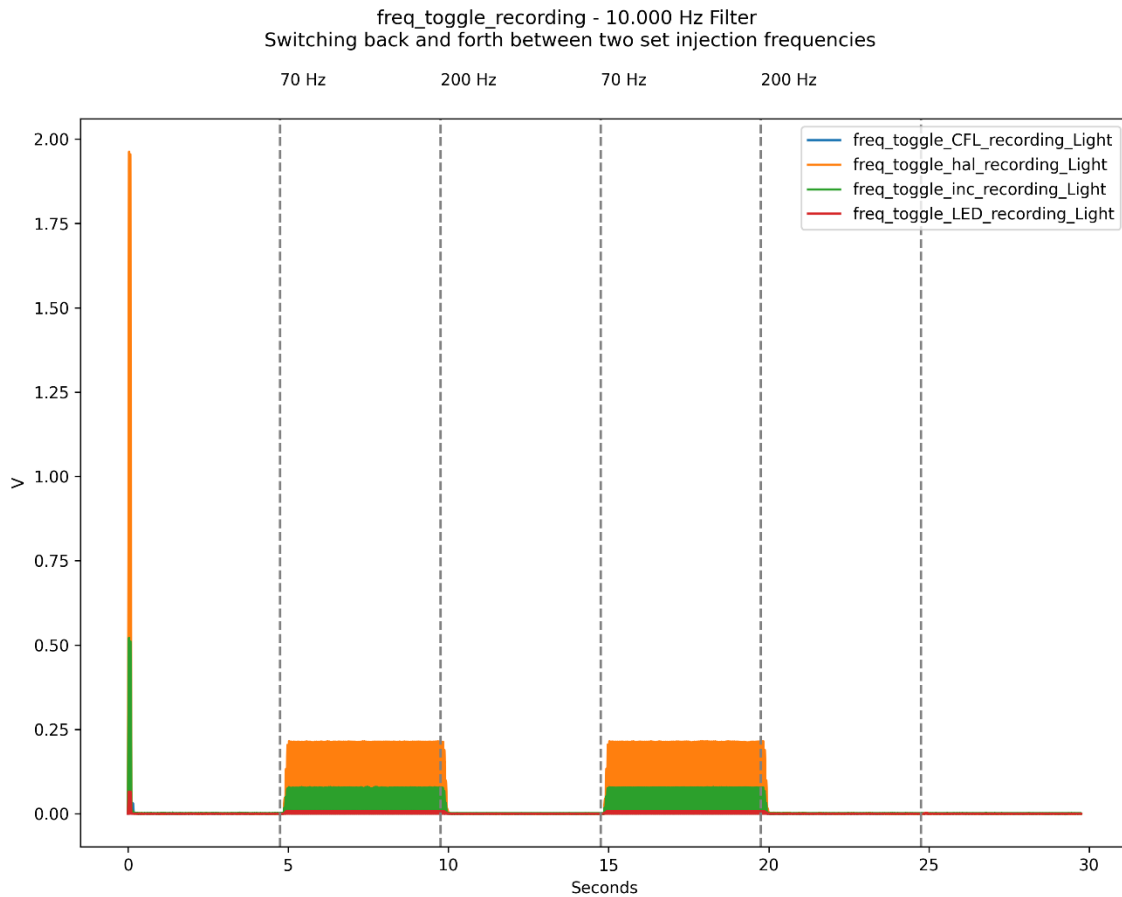


Figure 28 demonstrates several interesting attributes that are made all the more pronounced by the toggling behavior of the test. The first attribute of interest is the presence of many interharmonic components in the LED and CFL bulb outputs during the 200 Hz testing segments. The second notable feature of the above plot is the strong 10 Hz component that is present in all the bulbs during the 70 Hz injection windows. This provides an excellent example of how noise at one frequency can result in effects at very different frequencies than either the noise or the fundamental. This means that even noise that would normally be considered low or moderate risk according to the IEEE guidance in Section 2.4.5.3, can generate flicker behavior at high-risk frequencies.

5.3.3.4 Discrete Fourier Transform

The following two plots demonstrate the application of filters when plotting data. In this case, both figures show the application of a discrete Fourier transform (DFT) to highlight the presence of particular frequency components in the light data.

Figure 29: 10 Hz DFT for All Light Channels During Frequency Toggle Test



In Figure 29, all the light values are filtered to show 10 Hz components and are plotted on the same graph. As with the frequency sweep data, the lack of normalization makes direct comparison between the incandescent, halogen, CFL, and LED data difficult. However, a strong 10 Hz component can be easily seen in all the channels during the 70 Hz injection segments. That same 10 Hz component is not present during other points in the test.

Figure 30: 20 Hz DFT for Individual Light Channels During Frequency Toggle Test

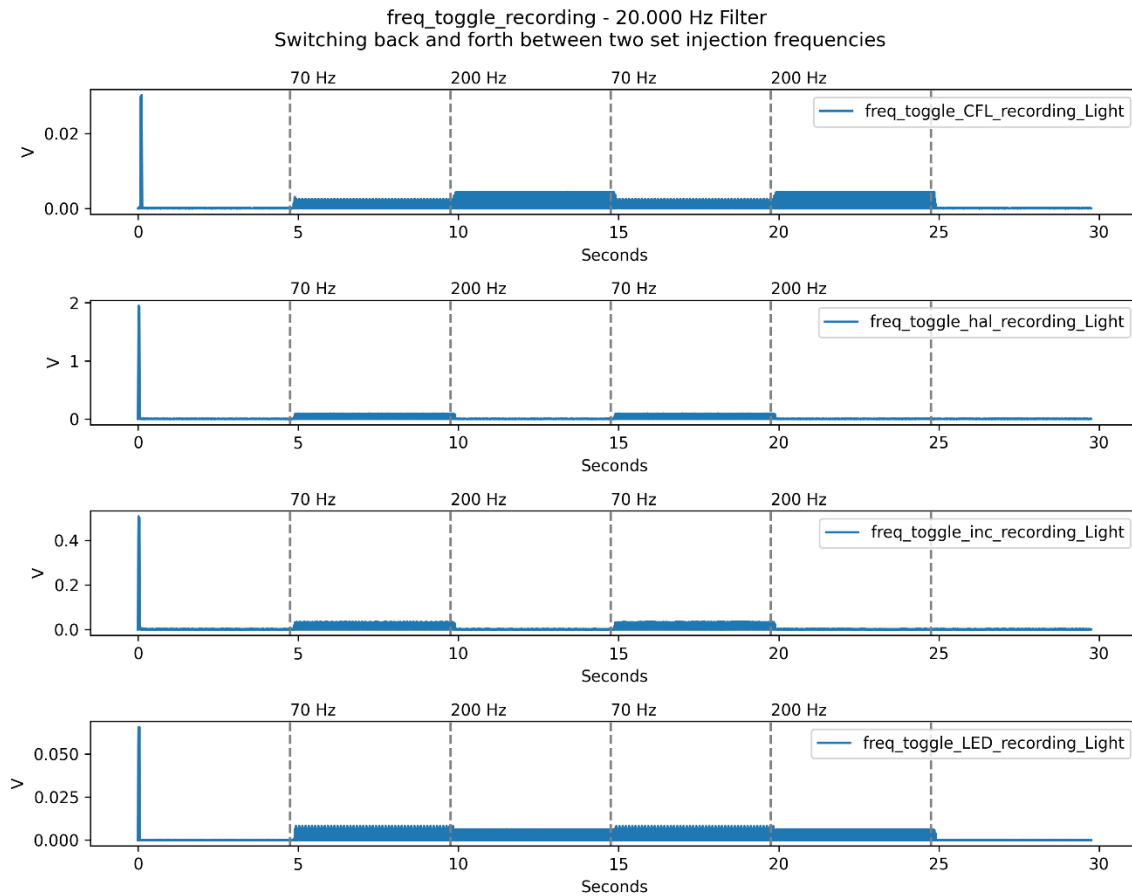


Figure 30 shows the result of a similar filtering process to Figure 29, but in this case each channel of light data is plotted separately, and the filter is set to show 20 Hz components instead of 10 Hz. The above plots show how the 70 Hz injected noise generates both 10 Hz and 20 Hz subharmonics, but the 200 Hz signal only injects 20 Hz. A more complete analysis and explanation relating to subharmonics and interharmonics will have to be saved for future work (see Section 6.3). However, the above plots clearly demonstrate the ability to capture and display a wide range of frequency effects.

5.3.4 Single Tone Injection

The frequency sweep and frequency toggle tests were focused on observing output changes for varying inputs. By contrast, the intention of the single tone injection tests was to get a better sense of the steady-state response of a bulb to a given input.

5.3.4.1 Test Description

Rather than one test with a variety of different frequencies, this sequence consisted of eighteen different ten-second tests, each one with a single injected frequency (i.e. tone). All the injected signals had the same magnitude, 5% of the fundamental. The list of injected frequencies is given below.

Table 8: List of Single Tone Injection Frequencies

• 8.3 Hz	• 53 Hz
• 8.8 Hz	• 67 Hz
• 10 Hz	• 70 Hz
• 13 Hz	• 80 Hz
• 15 Hz	• 90 Hz
• 20 Hz	• 100 Hz
• 30 Hz	• 120 Hz
• 40 Hz	• 150 Hz
• 50 Hz	• 180 Hz

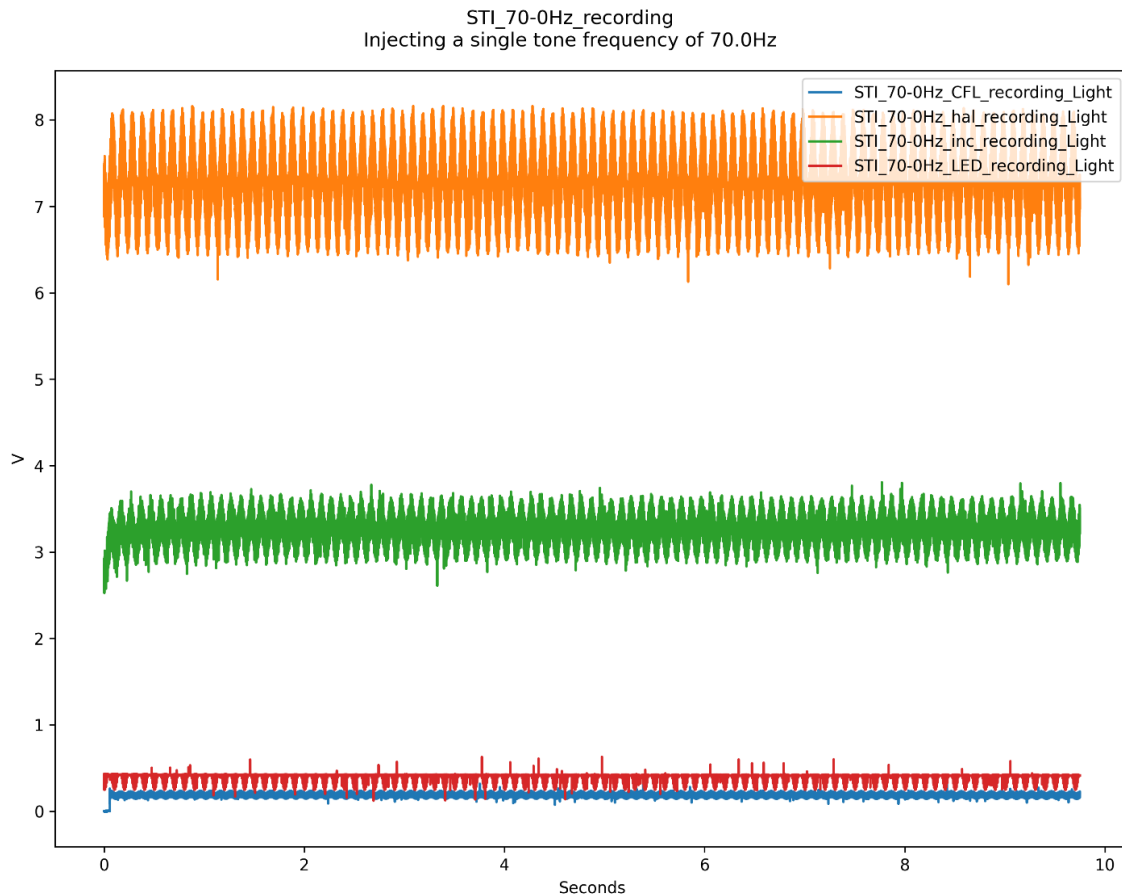
Running eighteen separate test sequences per bulb, as opposed to a single test for each bulb, presented a challenge when merging the data captures into a single file. The sheer number of channels involved (18 tests x 4 bulbs x 4 channels = 288 channels of data) made plotting all the values together infeasible. Instead, the plots below either feature the combined results from a single test frequency or are otherwise split up to show the response of a single bulb across all eighteen tests.

Some relevant output plots for this test sequence are shown in the sections below.

5.3.4.2 Time Domain Plots

Figure 31 shows the time domain light values for each bulb over the course of the 70 Hz test. The 70 Hz response was chosen for display due to the strong reaction at 70 Hz that was exhibited by the bulbs during the previous testing.

Figure 31: Time Domain Response to 70 Hz Injected Noise for All Bulb Light Channels

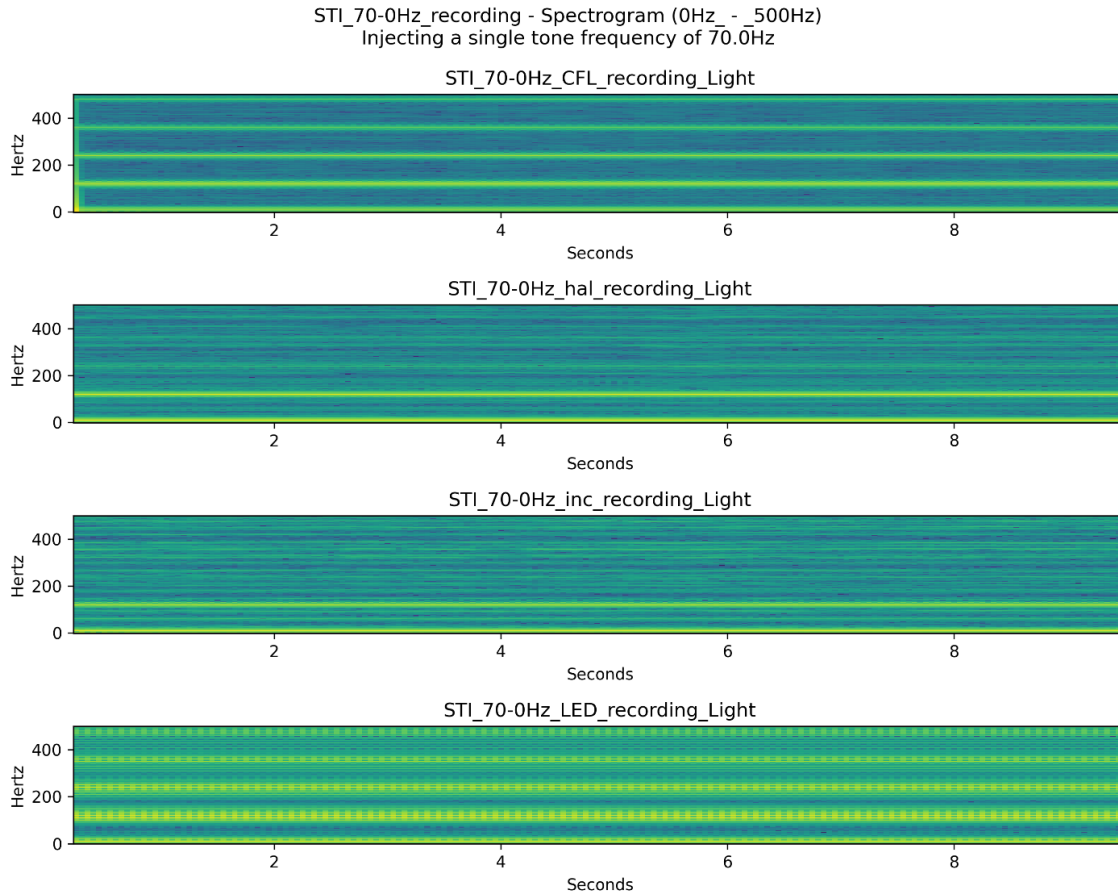


The above plot presents much the same information as was visible in the frequency sweep and frequency toggle tests. All the bulbs present a notable response to 70 Hz injected noise. One feature clearly visible in the above plot that was not quite as noticeable in previous plots is the apparent asymmetry of the LED output distortion. All the other bulbs have distortions that extend both above and below the average output value. The LED output, by contrast, has clear distortions below the average value, but has little to no distortion above the average. Further research is necessary to understand the cause of this asymmetric output behavior.

5.3.4.3 Spectrogram

Figure 32 shows the spectral content of each bulb's respective light output over the course of the 70 Hz injected noise test.

Figure 32: Spectral Response for All Light Channels During 70 Hz STI Test.



The two most notable features of Figure 32 are the clear banding visible in all of the captures and the wide range of noise present in the LED capture. The banding effect, where clear spans of harmonic content are visible in regularly repeating bands, is visible even in the incandescent and halogen plots. Visible harmonic effects in the incandescent and halogen plots have been substantially less common in the other tests, so the existence of visible harmonics for those bulbs is notable. The high noise level present in the LED plot is clearly noticeable and is likely related to the asymmetric distortion present in the time domain plot.

5.3.4.4 Frequency Domain

The following four plots show the frequency domain response of each bulb to the various input test frequencies. Comments and notable effects are documented below Figure 36.

Figure 33: Frequency Response of CFL Bulb Light Output to Different Injected Tones

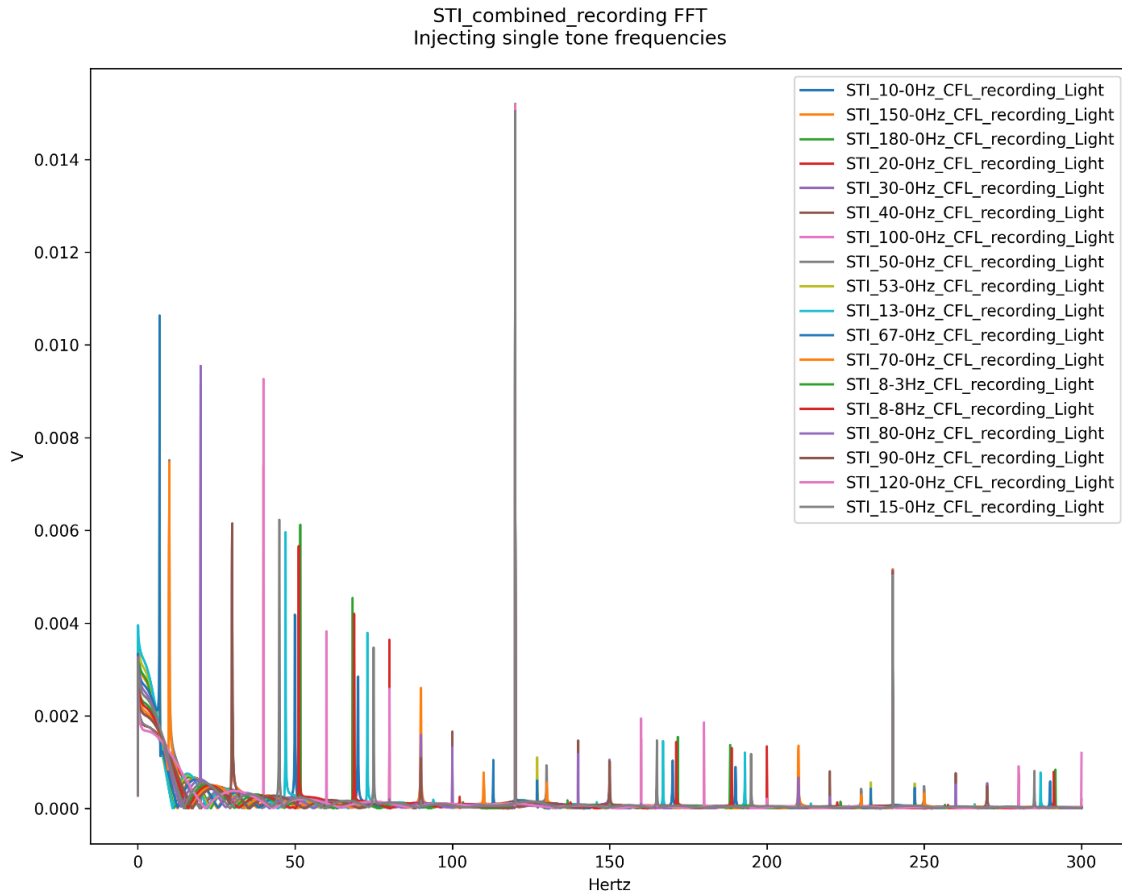


Figure 34: Frequency Response of Halogen Bulb Light Output to Different Injected Tones

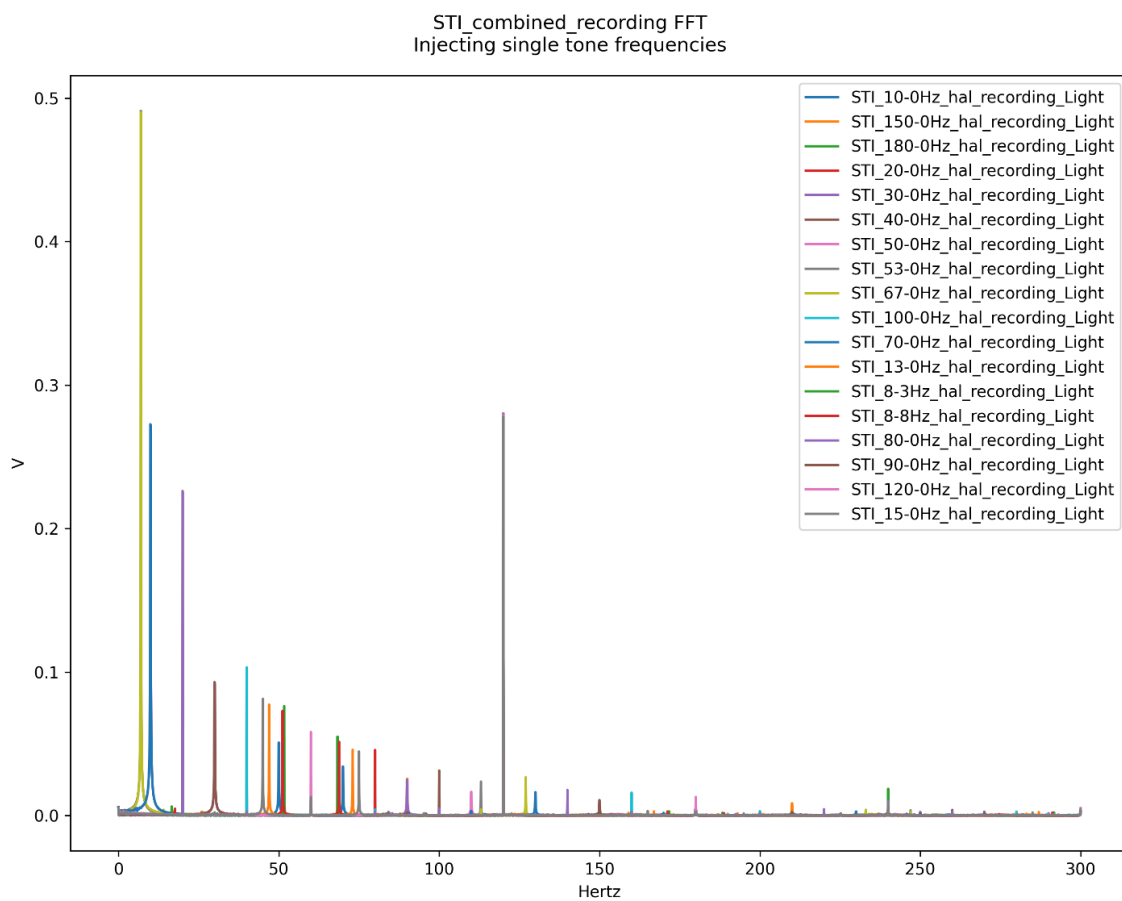


Figure 35: Frequency Response of Incandescent Bulb Light Output to Different Injected Tones

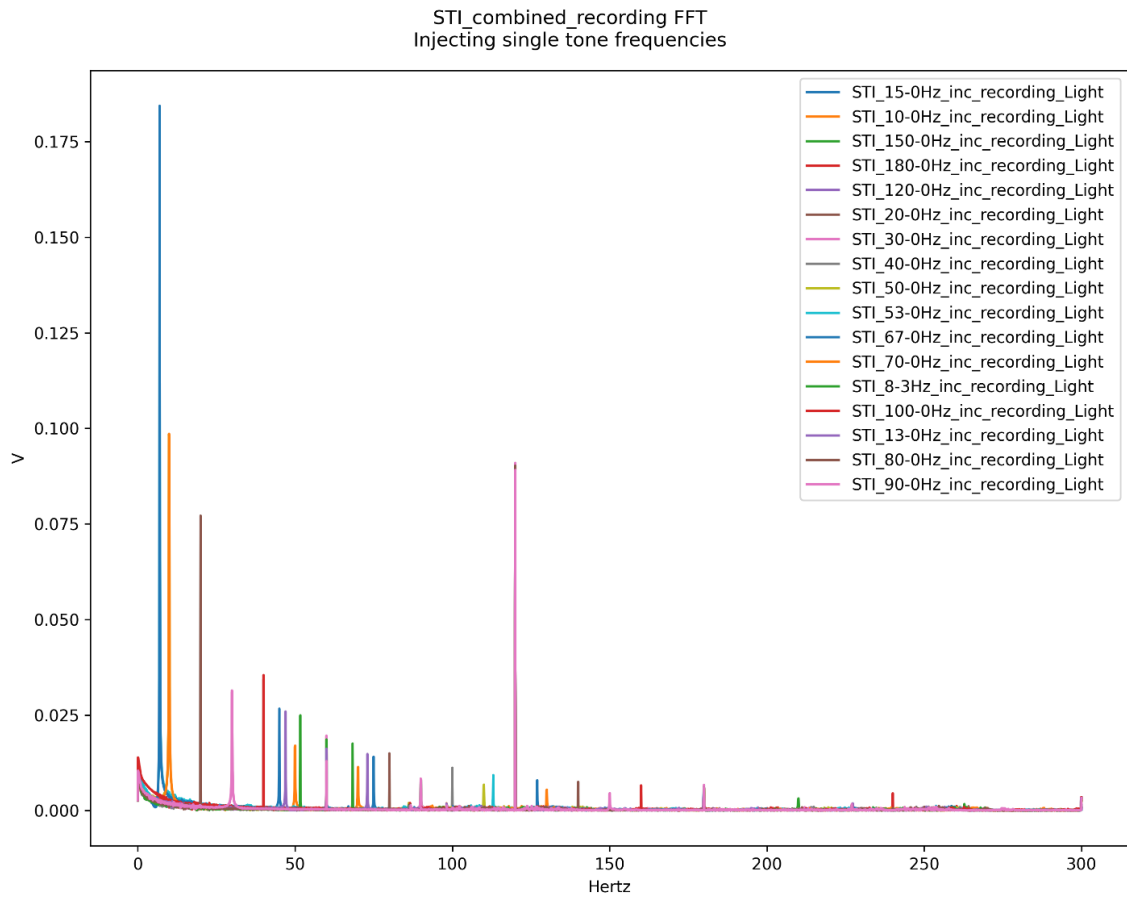


Figure 36: Frequency Response of LED Bulb Light Output to Different Injected Tones

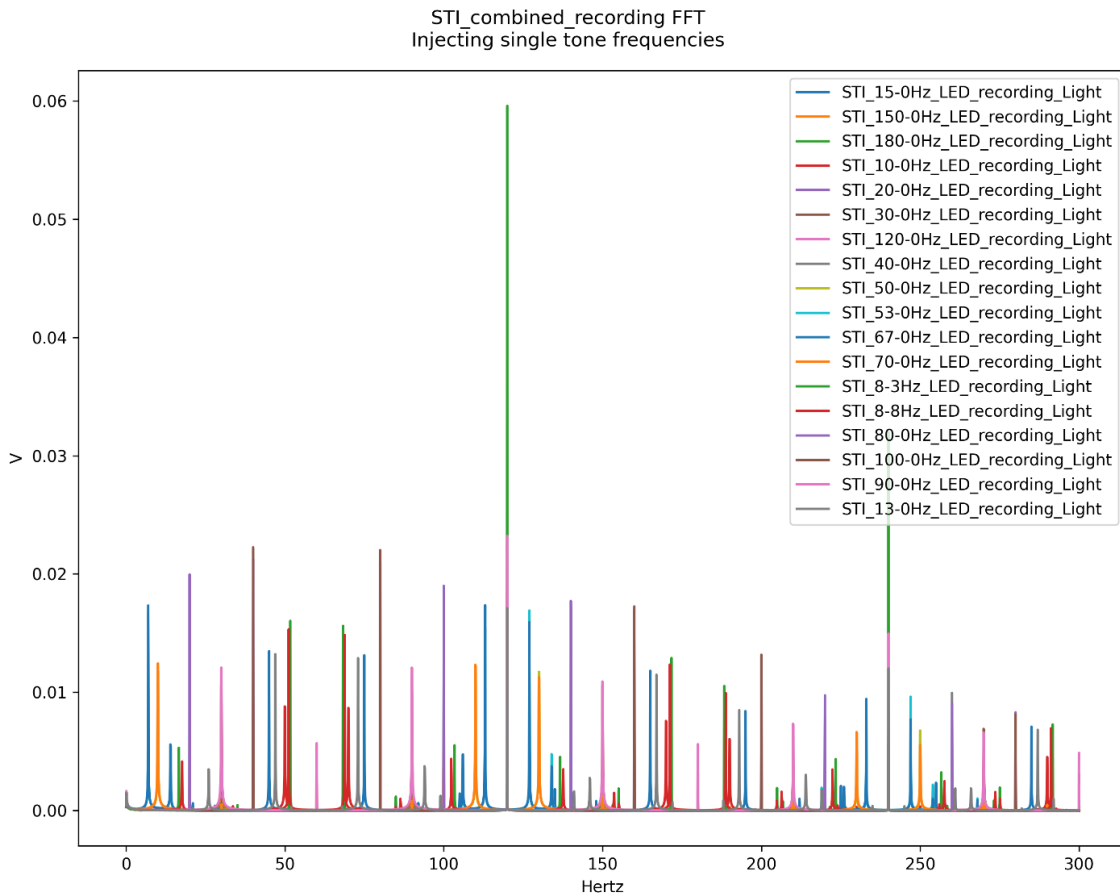


Figure 33-Figure 36 show a slightly different approach to capturing the frequency response of a given bulb than was attempted in the frequency sweep test. While the actual magnitudes of the various frequency components vary wildly from bulb to bulb (the peak value for the halogen bulb is nearly an order of magnitude higher than the peak value for the LED bulb), it can still be seen that the response shape is quite different from bulb to bulb. The incandescent and halogen bulbs have strong components at low frequencies that drop off rapidly as the frequency increases. By contrast, the frequency behavior of the LED bulb is much flatter than the other bulbs, but there are still notable harmonic elements at frequencies well above the point where the harmonic content of all the other bulbs is almost nothing. The above plots show another case where normalizing the data would allow for a more direct comparison between the various bulb output behaviors.

5.4 Conclusion

While the plots in the above sections were not intended to be an exhaustive or in-depth analysis of the output behaviors of the various bulbs, the figures do demonstrate the ability to programmatically generate, measure, analyze, and plot important quantities and values using the developed H5 toolchain. The figures also provide insight into interesting bulb behaviors, which can help guide future research. Most importantly, the figures justify and validate the development of both the test fixture and the toolchain that were the ultimate focus of this research. While there are some improvements, such as plot normalization, that could be made to improve the overall effectiveness of the H5 toolchain, the toolchain has been shown to be quite effective at capturing and displaying data.

Chapter 6: Summary, Conclusion, and Future Work

6.1 Summary

This thesis provided a basic background introduction into light measurement, flicker characteristics, risks associated with flicker, and IEEE guidance related to the limiting of flicker. The development of physical hardware and a test fixture setup were created, described, and documented. Primarily, this paper documented the development of a toolchain for programmatically generating, measuring, processing, and plotting data sets, with an emphasis on the tools being used for flicker analysis. Finally, examples were provided of using the toolchain to generate, capture, and plot the outputs from several different flicker tests. Though not exhaustive, the example outputs did provide insight into the frequency-dependent behaviors of several different light bulbs. Most importantly, the generated outputs clearly demonstrated the ability of the testbed and toolchain to generate test signals, measure and record those signals, analyze the recorded data, and provide outputs.

6.2 Conclusion

During the course of this research project, the goal of the research shifted from performing flicker analysis to developing the tools to perform the flicker analysis. The result was a toolchain that was clearly able to meet the identified needs of the research topic. The developed testbed and toolchain allowed for description-based signal generation, scripted test sequences, controlled data management and organization, and automatic analysis and plot generation. While the initial research goal still remains, the development of the H5 toolchain is a notable achievement that will hopefully provide great utility to the working group and also to SEL as a whole.

6.3 Future Work

6.3.1 Analyzing Flicker Characteristics of Various Bulb Types

The original goal of this research had been to gain an understanding of what sort of events on a power system were likely to cause undesirable or harmful levels of flicker in various bulb types. The intent was to see if there were any common elements present from bulb to bulb or if certain types of transients would be more likely than others to cause flicker. One of the key areas of future research is to continue with the original research intent of this thesis and analyze the flicker behavior of various bulbs.

6.3.2 Improving Test Fixture to Allow for More Accurate Energy Measurement

The current test fixture is only capable of measuring relative differences between the input voltage/current and the output voltage from the light sensor. A re-design of the fixture would allow for more precise measurement of the actual energy transfer process. Ideally the updated design would allow for the tests to account for the spectral response of the bulb, fixture, and sensor.

6.3.3 Ongoing Improvements to the H5 Toolchain

The long-term goal for the H5 toolchain is to have a consistent and versatile data capture, conversion, analysis, and plotting library that can be adopted by other portions of SEL for use in testing and validation. The tools are already being used for testing by other teams in the working group. In order to be ready for wider adoption, however, the toolchain will require continual refinement and adjustment. One example of a tool improvement would be the ability to normalize data during the plotting process, as was noted in Section 5.3.

6.3.4 Validate IEEE Flicker Guidance

IEEE Std 1789-2015 [13] provides guidance on how to analyze measured flicker behavior and map it to the scale provided in Figure 10. However, the nature of the guidance does not provide a clear way to handle flicker behavior that is transient in nature, or which consists of multiple, superimposed frequencies. In fact, the standard directly acknowledges the uncertainty of how to handle subharmonic and interharmonic components:

The recommended operating area of Figure 20 [Figure 10 in this paper] was derived assuming no subharmonics or interharmonics.

There is ongoing research on how to weight the harmonic components in the Fourier series that includes subharmonic and interharmonic frequencies. For low frequencies (<35 Hz to 40 Hz), the authors of IEEE Std 1453-2011 [B59], IEC 61000-4-15:2010 [B57], and IEC 61000-3-3:2013 [B56] are beginning to look at LED lamp flicker and plan in the future to write specifications about this subject in particular for LED lamp flicker due to voltage flicker. However, the IEC flickermeter remains applicable to the low frequency component; therefore, the Pst value approach could be carefully applied.

— *IEEE 1789-2015 Section 8.4 [13]*

In addition, the IEEE flickermeter guidance [23] deals with long term flicker levels, on the scale of minutes to hours. One important category of future work is to clearly understand the modeling and analysis of the IEEE guidance and to implement tools, filters, and plots capable of displaying the measured light output from the testing in a format congruent with the guidance provided by the IEEE.

6.3.5 Increased Current Draw on CFL and LED Bulbs When Exposed to Noise

Discovering the drastic increase in current draw from the CFL and LED bulbs during the frequency sweep test, as seen Figure 24, was an unexpected result. The observation that the current of the 11 W CFL exceeded that of the 100 W incandescent during that portion of the test sequence is quite notable. The frequency range of increased current (2000 – 8000 Hz for the CFL) is outside the applicable range of the IEEE flicker guidance [13], though other standards may apply. Further study could help determine the cause of the increased current draw, whether it increases the risk of component failure, how common it is for bulbs to experience noise in the relevant frequency range, and how to identify and mitigate noise and current effects.

6.3.6 Asymmetric Data on Some of The Captures

As was noted in Section 5.3.4.2, the LED light data in some of the captures displays asymmetric distortion in some cases. The cause of this asymmetry is currently unknown. A hypothesis is that the LED driver circuitry is limiting the current through the diodes to a certain level but allowing the output to dip during sags of the input voltage. Another hypothesis is that the support circuitry on the bulb is failing or mis-operating in an asymmetric manner—disassembly of failed bulbs has revealed that low-cost LED bulbs can fail due to the neutral connection heating enough to become de-soldered and disconnected, so asymmetric failure is a possibility. Further research is required in order to understand the nature of the observed asymmetric distortions.

Bibliography

- [1] Feit Electric, "100 Watt Incandescent A19," Feit Electric, 03 April 2017. [Online]. Available: https://www.feit.com/product/incandescentvibration_service_and_tuff_kotevibration_service100a-rs-tf-130/. [Accessed October 2022].
- [2] Ge Lighting, "GE Lighting PAR38 Halogen, Flood Light Bulbs, Warm White Spotlight, Indoor and Outdoor, 60-Watt, 1070 Lumen, Medium Base, 2-Pack," Amazon, [Online]. Available: <https://www.amazon.com/GE-Lighting-66279-Energy-Efficient-replacement/dp/B007V92RLI/>. [Accessed October 2022].
- [3] Walmart, "Great Value LED Light Bulb, 9W (60W Equivalent) A19 General Purpose Lamp E26 Medium Base, Non-dimmable, Soft White, 4-Pack," Walmart, [Online]. Available: <https://www.walmart.com/ip/Great-Value-LED-Light-Bulb-9W-60W-Equivalent-A19-General-Purpose-Lamp-E26-Medium-Base-Non-dimmable-Soft-White-4-Pack/51497369>. [Accessed October 2022].
- [4] GE Lighting, "GE Lighting 25195 Energy Smart spiral CFL 23-Watt, 1700-Lumen T3 Spiral Light Bulb with Medium Base, 1-Pack," [Online]. Available: <https://www.amazon.com/GE-Lighting-25195-23-Watt-1700-Lumen/dp/B002CYS5DG>. [Accessed 29 October 2022].
- [5] R. Cai, J. Cobben, J. Myrzik, J. Blom and W. Kling, "Flicker responses of different lamp types," *IET Generation, Transmission & Distribution*, vol. 3, no. 9, pp. 816 - 824, 2009.
- [6] M. Krajewski, "The great lightbulb conspiracy," *IEEE Spectrum*, vol. 51, no. 10, pp. 56-61, October 2014.
- [7] K. Chmielowiec, "Flicker effect of different types of light sources," in *11th International Conference on Electrical Power Quality and Utilisation*, Lisbon, Portugal, 2011.
- [8] G. M. Masters, *Renewable and Efficient Electric Power Systems*, 2nd ed., Hoboken, New Jersey: Wiley-IEEE Press, 2013.
- [9] Gigahertz-Optik, Inc., "Basics of Light Measurement," [Online]. Available: <https://light-measurement.com/tutorials-on-light-measurement/tutorials.pdf>. [Accessed July 2022].

- [10] RBW, "Understanding Color Temperature of LED lighting," RBW, 29 May 2013. [Online]. Available: <https://rbw.com/blog/understanding-color-temperature-of-led-lighting>. [Accessed October 2022].
- [11] M. Hansen, L. Davis, T. Clark, M. Duffy, P. Gaines, E. Haugaard, M. Pattison, C. Robinson, S. Sarraf, Driel and W. van Driel, "LED Luminaire Reliability: Impact of Color Shift," U.S. Department of Energy, Washington DC, 2017.
- [12] J. Priest, "The DIY Decorator's Eco-Friendly Lighting Dilemma," housecraft, 30 September 2012. [Online]. Available: <http://housecraft.ca/eco-friendly-lighting-colour-rendering-index-and-colour-temperature/>. [Accessed August 2022].
- [13] IEEE, 1789-2015 - IEEE Recommended Practices for Modulating Current in High-Brightness LEDs for Mitigating Health Risks to Viewers, IEEE, 2015.
- [14] British Electrical and Allied Industries Research Association, "The production of flicker in electric lamps by cyclic irregularity in the voltage," *Journal of the Institution of Electrical Engineers*, vol. 64, no. 358, pp. 1090 - 1092, 1926 .
- [15] S. Griscom, "Lamp Flicker on Power Systems," in *Electrical Transmission and Distribution Reference Book*, Raleigh, North Carolina, ABB Power T&D Company Inc., 1997, pp. 719-740.
- [16] B. Lehman, A. Wilkins, S. Berman, M. Poplawski and N. J. Miller, "Proposing measures of flicker in the low frequencies for lighting applications," in *2011 IEEE Energy Conversion Congress and Exposition*, Phoenix, AZ, USA, 2011.
- [17] M. B. Kobav, "Flicker experimental set up and visual perception of flicker," in *2018 Seventh Balkan Conference on Lighting (BalkanLight)*, Varna, Bulgaria, 2018.
- [18] T. Kim, M. Rylander, E. J. Powers, W. M. Grady and A. Arapostathis, "LED Lamp Flicker Caused by Interharmonics," in *2008 IEEE Instrumentation and Measurement Technology Conference*, Victoria, BC, Canada, 2008.
- [19] B. Lehman and A. J. Wilkins, "Designing to Mitigate Effects of Flicker in LED Lighting: Reducing risks to health and safety," *IEEE Power Electronics Magazine*, vol. 1, no. 3, pp. 18-26, 2014 .

- [20] J. Bullough, K. S. Hickcox, T. Klein, A. Lok and N. Narendran, "Detection and acceptability of stroboscopic effects from flicker," *Lighting Research & Technology*, vol. 44, no. 4, pp. 477-483, 2011.
- [21] O. Rahman, S. Elphick, K. M. Muttaqi and J. David, "Investigation of LED Lighting Performance in the Presence of Ripple Injection Load Control Signals," *IEEE Transactions on Industry Applications*, vol. 55, no. 5, pp. 5436 - 5444, 2019.
- [22] V. B. Virulkar and M. V. Aware, "Modeling and simulation of flicker due to interharmonics," in *India International Conference on Power Electronics 2010 (IICPE2010)*, New Delhi, India, 2011.
- [23] IEEE, "IEEE Recommended Practice for the Analysis of Fluctuating Installations on Power Systems," *IEEE Std 1453-2015 (Revision of IEEE Std 1453-2011)*, pp. 1-74, 2015.
- [24] J. Drapela and J. Slezingr, "Design and utilization of a light flickermeter," in *2012 IEEE International Workshop on Applied Measurements for Power Systems (AMPS) Proceedings*, Aachen, Germany, 2012.
- [25] K. R. Shailesh and T. Shailesh, "Review of photometric flicker metrics and measurement methods for LED lighting," in *2017 4th International Conference on Advanced Computing and Communication Systems (ICACCS)*, Coimbatore, India, 2017.
- [26] J. Drapela, R. Langella, A. Testa, A. J. Collin, X. Xu and S. Z. Djokic, "Experimental evaluation and classification of LED lamps for light flicker sensitivity," in *2018 18th International Conference on Harmonics and Quality of Power (ICHQP)*, Ljubljana, Slovenia, 2018.
- [27] S. Sakar, S. Rönnerberg and M. H. J. Bollen, "Immunity test of LED lamps based on IEC 61000-4 19 and unexpected consequence," in *2018 18th International Conference on Harmonics and Quality of Power (ICHQP)*, Ljubljana, Slovenia, 2018.
- [28] National Instruments, "CompactDAQ Systems," National Instruments, 25 August 2022. [Online]. Available: <https://www.ni.com/en-us/shop/compactdaq.html>. [Accessed 27 October 2022].

- [29] National Instruments, "NI-9263 Datasheet," National Instruments, 03 May 2022. [Online]. Available: <https://www.ni.com/docs/en-US/bundle/ni-9263-specs/page/specs.html>. [Accessed October 2022].
- [30] National Instruments, "NI 9215 Specifications," National Instruments, 19 December 2021. [Online]. Available: <https://www.ni.com/docs/en-US/bundle/ni-9215-specs/page/specs.html>. [Accessed October 2022].
- [31] National Instruments, "cDAQ-9174 Specifications," National Instruments, 16 September 2022. [Online]. Available: <https://www.ni.com/docs/en-US/bundle/cdaq-9174-specs/page/specs.html>. [Accessed October 2022].
- [32] AE Techron Inc, "LV 3620 Operators's Manual," 01 January 2001. [Online]. Available: <https://www.aetechron.com/pdf/3620manual.pdf>.
- [33] Pico Technology, "25 MHz 700 V differential oscilloscope probe 10:1/100:1," Pico Technology, 2020. [Online]. Available: <https://www.picotech.com/accessories/active-differential-high-voltage/25-mhz-700-v-differential-probe>. [Accessed October 2022].
- [34] Teledyne LeCroy, "AP031," Digi-Key, 2022. [Online]. Available: <https://www.digkey.com/en/products/detail/teledyne-lecroy/AP031/3961353>. [Accessed October 2022].
- [35] Flex-Core Inc., "AC Micro Clamp Current Transformer," Flex Core, 2022. [Online]. Available: <https://www.flex-core.com/products/current-transformers/low-voltage-current-transformers/low-voltage-split-core-current-transformers/m1-ac-micro-clamp-current-transformer/>. [Accessed October 2022].
- [36] Fluke, "Fluke 324 True-RMS Clamp Meter with Temperature & Capacitance," Fluke Corporation, October 2022. [Online]. Available: <https://www.fluke.com/en-us/product/electrical-testing/clamp-meters/fluke-324>. [Accessed October 2022].
- [37] Thorlabs, "PDA100A2 Si Switchable Gain Detector User Guide," 21 April 2020. [Online]. Available: <https://www.thorlabs.com/thorproduct.cfm?partnumber=PDA100A2>. [Accessed 2020].

- [38] GE Lighting, "GE Lighting 47486 Energy Smart CFL 11 (40-watt Replacement) 500-Lumen A17 Light Bulb with Medium Base, 1-Pack, Soft White Long Life," [Online]. Available: <https://www.amazon.com/GE-Lighting-47486-replacement-500-Lumen/dp/B002YELZMW>. [Accessed October 2022].
- [39] Allied Moulded Products, Inc., "AM1206RT," InfoStream Solutions, October 2022. [Online]. Available: <https://www.alliedmoulded.com/product/am1206rt/>.
- [40] D. Daigle, "SELDAQ and NIPlay (Unpublished Software)," Schweitzer Engineering Laboratories, Inc., Pullman, 2018.
- [41] Microsoft, "Excel specifications and limits," [Online]. Available: <https://support.microsoft.com/en-us/office/excel-specifications-and-limits-1672b34d-7043-467e-8e27-269d656771c3>. [Accessed 24 October 2022].
- [42] E. A. Bruford, B. Braschi, P. Denny, T. E. M. Jones, R. L. Seal and S. Tweedie, "Guidelines for human gene nomenclature," *Nature Genetics*, no. 52, p. 754–758, 2020.
- [43] The HDF Group, "HDF5," The HDF Group, 20 September 2022. [Online]. Available: <https://portal.hdfgroup.org/display/HDF5/HDF5>. [Accessed 15 October 2022].
- [44] K. Graal, B. Holdsworth and L. Brennan-Shiel, "Stone Soup, A story for World Food Day," Unilever, 2008. [Online]. Available: <https://documents.wfp.org/stellent/groups/public/documents/webcontent/wfp202398.pdf>. [Accessed October 2022].
- [45] C. G. Rieger, "Resilient control systems Practical metrics basis for defining mission impact," in *2014 7th International Symposium on Resilient Control Systems (ISRCS)*, Denver, CO, USA, 2014.

Appendix A: The H5 Tool library

A.1 H5 Model

The following example shows the type of information stored in the H5Model.

A.1.1 Usage Example

- Run the following command

```
`python -m h5model <HDF5_FILE_PATH>`
```

- These commands will print something like the following

```
d:\Projects\WhaleOil\results\STI\STI_67-0Hz_inc.h5:
  __type__: h5model.models.PlottableDataListFileWithMetaData
  __version__: 0.1
  name: STI_67-0Hz
  description: Injecting a single tone frequency of 67.0Hz
  username: ericjohn
  filename:
D:\Projects\WhaleOil\results\freq_sweep\freq_sweep_incandescent.json
  timestamp: 1664468797.571495
  history:
    history0:
      __type__: h5model.models.H5FileMetaData
      __version__: 0.1
      timestamp: 1664469414.519704
      username: ericjohn
      filename:
D:\Projects\WhaleOil\results\freq_sweep\freq_sweep_incandescent.json
  message: Ran experiment from
D:\Projects\WhaleOil\results\freq_sweep\freq_sweep_incandescent.json
  plottable_data:
    h5model.models.PlottableDataset:
      __type__: h5model.models.PlottableDataset
      __version__: 0.1
      chunks: None
      maxshape: (1, 1000000)
      name: STI_67-0Hz_signal
      description: Injecting a single tone frequency of 67.0Hz
      duration: 10.0
      sample_rate: 100000
      sample_count: 1000000
```

```

channel_count: 1
channel_names: ['Vgen']
x_axis_labels: ['Seconds']
y_axis_labels: ['Volts']
data:
  dtype: float64
  shape: (1, 1000000)
  maxshape: (1, 1000000)
  chunks: None
h5model.models.PlottableDataset:
  __type__: h5model.models.PlottableDataset
  __version__: 0.1
  chunks: (4, 20000)
  maxshape: (4, 1000000)
  name: STI_67-0Hz_inc_recording
  description: Injecting a single tone frequency of 67.0Hz
  duration: 10.0
  sample_rate: 100000
  sample_count: 1000000
  channel_count: 4
  channel_names: ['Vbulb', 'Cbulb', 'Light', 'Vin']
  x_axis_labels: ['Seconds', 'Seconds', 'Seconds', 'Seconds']
  y_axis_labels: ['V', 'A', 'V', 'V']
  data:
    dtype: float64
    shape: (4, 1000000)
    maxshape: (4, 1000000)
    chunks: (4, 20000)

```

A.1.1. File Components

A.1.1.1. File Metadata

This section includes basic information about the file as a whole, including the model name, type, and description. It also includes some automatically generated values, such as the username of the person who called the H5model script, and the current Unix timestamp.

A.1.1.2. History

This is a list of file metadata elements that exists to keep track of ways the model file may have been modified over time. It logs the username of the person interacting with the model, as well as the timestamp for when the modification happened, and a description of what may have changed/or what action occurred.

A.1.1.3. Plottable Data

List of plottable datasets present in the model file.

A.1.1.4. Plottable Dataset

This is where the actual data values are stored. It includes the name and description of the data set, as well as the sample rate, duration, sample count, channel count, channel names, axis/unit names, and the NumPy array containing the raw data values.

A.2 H5 Signal Generator

An example signal.JSON is shown below.

The template signal file can be generated by running the following command from the command line

```
python -m h5signalgen --create_template YOUR_SIGNAL_FILE_JSON_PATH
```

This will generate a default signal template file, which can then be modified and run through the signal generator tool to create an HDF5 file containing the specified signal set.

A.2.1 Example Signal Description File

Figure 37: Example Signal.JSON Template

```
{
  "name": "no_file_name",
  "description": "no_file_description",
  "filename": "PATH_TO_WRITE_HDF5_FILE",
  "history": [],
  "signals": [
    {
      "name": "THE_NAME_TO_BE_USED_FOR_THIS_CHANNEL_OF_DATA",
      "description": "no_signal_description",
      "components": [
        {
          "name":
"OPTIONAL_NAME_FOR_YOUR_USE_BUT_IGNORED_ELSEWHERE",
          "frequency": 0.0,
          "phase_offset_degrees": 0.0,
          "start_seconds": 0.0,
          "duration_seconds": 0.0,
          "add_noise": false,
          "noise_decibels": -300.0,
          "amplitude": 1.0
        },
        {
          "name": "OPTIONAL_SECOND_SIGNAL_TO_BE_ADDED_INTO_FIRST",
          "frequency": 0.0,
          "phase_offset_degrees": 0.0,
          "start_seconds": 0.0,
          "duration_seconds": 0.0,
          "add_noise": false,
          "noise_decibels": -300.0,
          "amplitude": 1.0
        }
      ]
    },
    {
      "units": "VOLTS_AMPS_ETC_USED_IN_PLOTS",
      "sample_rate": 1
    }
  ]
}
```